

REPORT DOCUMENTATION PAGE

*Form Approved
OMB No. 0704-0188*

Public reporting burden for this collection of information is estimated to average 1 hour per response, including the time for reviewing instructions, searching existing data sources, gathering and maintaining the data needed, and completing and reviewing this collection of information. Send comments regarding this burden estimate or any other aspect of this collection of information, including suggestions for reducing this burden to Department of Defense, Washington Headquarters Services, Directorate for Information Operations and Reports (0704-0188), 1215 Jefferson Davis Highway, Suite 1204, Arlington, VA 22202-4302. Respondents should be aware that notwithstanding any other provision of law, no person shall be subject to any penalty for failing to comply with a collection of information if it does not display a currently valid OMB control number. PLEASE DO NOT RETURN YOUR FORM TO THE ABOVE ADDRESS.

| | | | | |
|--|--|-------------------------------------|---|---|
| 1. REPORT DATE (DD-MM-YYYY) 07-11-2006 | 2. REPORT TYPE Journal Article | 3. DATES COVERED (From - To) | | |
| 4. TITLE AND SUBTITLE Atomization of Wall-Bounded Two-Phase Flows (Preprint) | | | 5a. CONTRACT NUMBER | |
| | | | 5b. GRANT NUMBER | |
| | | | 5c. PROGRAM ELEMENT NUMBER | |
| 6. AUTHOR(S) Malissa D.A. Lightfoot (AFRL/PRSA) | | | 5d. PROJECT NUMBER | |
| | | | 5e. TASK NUMBER 50260538 | |
| | | | 5f. WORK UNIT NUMBER | |
| 7. PERFORMING ORGANIZATION NAME(S) AND ADDRESS(ES) Air Force Research Laboratory (AFMC) AFRL/PRSA 10 E. Saturn Boulevard Edwards AFB CA 93524-7680 | | | 8. PERFORMING ORGANIZATION REPORT NUMBER AFRL-PR-ED-JA-2006-451 | |
| | | | 10. SPONSOR/MONITOR'S ACRONYM(S) | |
| 9. SPONSORING / MONITORING AGENCY NAME(S) AND ADDRESS(ES) Air Force Research Laboratory (AFMC) AFRL/PRS 5 Pollux Drive Edwards AFB CA 93524-7048 | | | 11. SPONSOR/MONITOR'S NUMBER(S) AFRL-PR-ED-JA-2006-451 | |
| | | | 12. DISTRIBUTION / AVAILABILITY STATEMENT Approved for public release; distribution unlimited (AFRL-ERS-PAS-2006-285) | |
| 13. SUPPLEMENTARY NOTES Submitted to Atomization and Sprays | | | | |
| 14. ABSTRACT The current understanding of droplet generation processes from liquid films is reviewed. Films are defined as liquids with one free and one wall-bound surface. In many of the systems where films occur, atomization is an undesirable side-effect of the two-phase flow. The motivation for this study, however, is a process where atomization from the film is the goal—an injector used in a rocket combustion chamber. Because atomization is often unwanted in film configurations, few studies focus on the mechanisms that cause atomization in this set-up. The large body of literature on the atomization of jets and sheets is, therefore, utilized in this review. Similarities and differences between the geometries are discussed when applicable. Generally, the atomization is considered to involve two steps: the creation of a disturbance on the film surface and the breakdown of this disturbance into droplets. Prompt Atomization, where atomization occurs directly at a nozzle exit, is also briefly discussed. Several atomization mechanisms are identified from the literature. Theoretical descriptions are given where available, but, due to limitations in the current understanding and the complexity of the atomization process, these are somewhat incomplete. Consequently, important nondimensional groupings and a selection of empirical correlations are also given to aid in the understanding of film atomization. | | | | |
| 15. SUBJECT TERMS | | | | |
| 16. SECURITY CLASSIFICATION OF: | | 17. LIMITATION OF ABSTRACT | 18. NUMBER OF PAGES | 19a. NAME OF RESPONSIBLE PERSON Dr. Stephen Danczyk |
| a. REPORT Unclassified | b. ABSTRACT Unclassified | c. THIS PAGE Unclassified | SAR 64 | 19b. TELEPHONE NUMBER (include area code) N/A |

Atomization of Wall-Bounded Two-Phase Flows (Preprint)

Malissa D.A. Lightfoot
Air Force Research Laboratory
10 East Saturn Blvd.
Edwards AFB, CA 93524-7660

Abstract

The current understanding of droplet generation processes from liquid films is reviewed. Films are defined as liquids with one free and one wall-bound surface. In many of the systems where films occur, atomization is an undesirable side-effect of the two-phase flow. The motivation for this study, however, is a process where atomization from the film is the goal—an injector used in a rocket combustion chamber. Because atomization is often unwanted in film configurations, few studies focus on the mechanisms that cause atomization in this set-up. The large body of literature on the atomization of jets and sheets is, therefore, utilized in this review. Similarities and differences between the geometries are discussed when applicable. Generally, the atomization is considered to involve two steps: the creation of a disturbance on the film surface and the breakdown of this disturbance into droplets. Prompt Atomization, where atomization occurs directly at a nozzle exit, is also briefly discussed. Several atomization mechanisms are identified from the literature. Theoretical descriptions are given where available, but, due to limitations in the current understanding and the complexity of the atomization process, these are somewhat incomplete. Consequently, important nondimensional groupings and a selection of empirical correlations are also given to aid in the understanding of film atomization.

I. Introduction

Atomization plays an important role in processes across many different industries. From the production of powdered metals to the functioning of a gasoline engine, from rocket engines to the delivery of medications and beyond, the breakup of a liquid into droplets is of key importance. Atomization also occurs as a side-effect of some operations, such as droplet production from the bow sheets of ships and entrainment of liquid in cooling tubes. Due to its commonality throughout a wide range of industries, atomization is an oft-studied phenomenon. Also not surprising is the vast array of devices that have been developed to accomplish and study atomization. Categorization of these devices (and operations involving atomization) by the liquid's geometric configuration during breakup can facilitate an understanding of this complex phenomenon. Here atomization configurations are broadly classified into one of three groups: jet, sheet or film.

In jet atomization the liquid is introduced as a cylindrical stream (Fig. 1a). This stream may be subjected to a coflowing or cross-flowing gas stream or it may be introduced into a quiescent environment. Sheet atomization is characterized by a stream of liquid that has two free surfaces. The sheet may be flat or axisymmetric (Figs. 1b and 1c, respectively). It may be subjected to an imposed gas velocity on either of its sides, both of its sides or neither side. Finally, a film is similar to a sheet, but is bounded on one side by a wall; the other side may or may not be subjected to an imposed gas flow. Films may have several geometries, but the most common in atomization processes are flat and annular (Figs. 1d and 1e, respectively). Note that the above nomenclature differs somewhat from that commonly found in the literature, where sheet, film and occasionally jet are used interchangeably [1, 2]. To avoid confusion and clarify

the following discussions the preceding definitions will be used throughout this paper: a sheet has two free surfaces while a film has one wall-bounded and one free surface; a jet has only one surface and it is a free surface.

The physical processes that lead to the disintegration of a liquid or the formation of droplets from its surface are termed atomization mechanisms. The breakup of jets, sheets and films occurs due to the complex interaction of several forces: aerodynamic, viscous, surface tension and inertial, for example [3-6]. The absolute and relative values of these forces as the atomization events progress determine the mechanisms involved. Knowledge of the mechanisms allows the development of a quantitative description of the spray—droplet size, distribution and velocity, for example. In reality, however, uncertainty about the exact mechanisms involved remains; plus, even if the processes are understood, they are often too complex to fully describe in a quantitative way. Nevertheless, a knowledge of the operable atomization mechanism(s) is important as it leads to the definition of specific atomization regimes, implies qualitative aspects of the resulting spray, highlights the similarities of various processes and suggests relevant scaling laws. Scaling laws are particularly important in some atomization applications, such as rocket engines and powdered metal production, where full-scale tests at operational pressures and/or temperatures can be costly and make measurements difficult. A solid understanding of the physics involved in the breakup process, therefore, helps to focus experiments and ground correlations as well as directing the development of new atomizer concepts. Atomization mechanisms vary somewhat between the three different geometries listed above (jet, sheet and film) because the relative importance of individual forces differs for each configuration [6, 7]. However, many similarities are found between the configurations [2, 7].

The motivation of this work is the recent studies of a rocket injector where atomization occurs from an annular film [8-10]. The main focus of this review paper, then, is the atomization mechanisms of films in parallel flows. Liquid film flows and atomization are found in bow sheets on ships, cooling tubes and towers, water chutes and spillways, a select group of atomizers and elsewhere. The main body of atomizer literature deals with jets or sheets as the majority of atomizers utilize these configurations. Comparatively little research exists on atomization mechanisms in the film configuration. Consequently, the summary of film atomization mechanisms will be predicated on brief reviews of the basic atomization regimes of jets and sheets. Some experimental studies have shown marked similarities in droplet production throughout jets, sheets and films ([2], for example); the similarities and differences between the geometries will be emphasized. The following section covers the atomization regimes of these three geometries; the regimes are specifically chosen to emphasize the similarities between the configurations. A brief discussion of atomizers that do not easily fit into these three main categories, e.g. effervescent atomizers, is also given here. In addition to stressing similarities, the review of regimes will be used to set the stage for the subsequent discussion of specific atomization mechanisms and submechanisms. Following a presentation of these mechanisms quantitative descriptions will be given for some of the mechanisms as available in the literature. As will be illustrated, solid quantitative descriptions and understanding of many atomization mechanisms is lacking, so this final section will also present important dimensionless groups and a brief selection of empirical correlations determined from experimental investigations. Due to the complexity and subsequent incompleteness of descriptions available in the literature, this paper is meant not only to review existent theories and literature, but to encourage and direct future research; consequently, current shortfalls of knowledge will be highlighted.

II. Atomization Regimes

A. Jets

This section presents a much abbreviated look at the atomization regimes of jets with an eye towards possible mechanisms in film atomization. For a more thorough review of jet atomization the reader is referred to the influential book by Lefebvre [5] or the review articles of Lin and Reitz [11] (jets in quiescent environments) Lasheras and Hopfinger [12] (jets in coflow), Margason [13] (jets in cross-flow) and Sallam, Dai and Faeth [14] (turbulent jets). As part of the abridgement of this subject, jets in cross-flow will not be addressed—this configuration is unrealistic in film atomization and is, therefore, not considered to further the agenda of this paper.

Experimental findings suggest three main regimes for jet atomization [12, 15, 16]: Rayleigh mode, Surface Breakup (Taylor mode) and Prompt Atomization. Generalized diagrams of each regime are given in Fig. 2. In the Rayleigh mode hydrodynamic instabilities produced by surface tension cause the jet surface to undulate [16]. Eventually the instabilities become large and the liquid column narrows to the point that a droplet is formed. These surface-tension-driven instabilities may be augmented by aerodynamic effects, as in the first wind-induced breakup mode [11], or liquid turbulence [17]. In sheets and films the liquid-gas surface tension is generally not destabilizing, but a similar atomization regime exists. The Surface Breakup regime is characterized by disturbances (waves, ligaments) on the surface of the jet. These disturbances are small compared with the jet diameter and may be caused by liquid turbulence [18], hydrodynamic instabilities [16] or the interaction of vortices in the gas phase [19]. Various mechanisms, discussed in the Atomization Mechanisms section, cause these protuberances to become droplets. This regime is sometimes referred to as the Taylor mode or second wind-induced breakup mode. Finally, in the Prompt Atomization regime disintegration starts at the nozzle exit [11, 15]. An extensive set of experiments by Reitz and Bracco [15] examined a number of posited atomization mechanisms responsible for Prompt Atomization of jets and found that none of the speculated mechanisms could account for all of the observed experimental behavior. Note that these regimes commonly follow each other in the order presented as the liquid and/or gas velocity increases.

To highlight the generality of these regimes consider the turbulent jet work of Sallam et al. [14] wherein three turbulent jet regimes are identified: a weakly-turbulent Rayleigh-Like mode, a Surface Breakup (primary-column breakup) mode and an Aerodynamic Bag/Shear Breakup mode. In the Rayleigh-Like mode instabilities are enhanced by the turbulence, but the behavior is basically identical to the classic Rayleigh-breakup mode [14]. Again, this is an instability phenomenon mainly driven by surface tension. In the Surface Breakup mode, the main mode of turbulent breakup, turbulence causes surface protrusions which break down into droplets; this mode is directly related to modes seen in sheet and film atomization and will be discussed in depth in the Atomization Mechanisms section. The Aerodynamic Bag/Shear Breakup mode is characterized by whole jet oscillations and large departures from the mean flow direction; consequently, breakup is accomplished by mechanisms similar to those of a jet in cross-flow [14]. Since a film could not oscillate as a whole this mode is not discussed further. (Again, Margason [13] presents a good review of jets in cross-flow.) Clearly the modes found for turbulent jets fit into the parallel/no-flow regimes discussed above or into cross-flow regimes not discussed here.

B. Sheets

The breakup of liquid jets and sheets differ in various fundamental ways. Most notably, surface tension is stabilizing in sheets with Weber numbers greater than some critical value, which is dependent on flow properties and conditions [7]; conditions in almost all atomizers have Weber numbers exceeding this critical value. Aerodynamic forces are of great importance in nearly all sheet breakup processes, with the exception of breakup due to liquid turbulence at sufficiently high liquid-to-gas density ratios [17, 20]; contrastingly, aerodynamic forces are secondary in the Rayleigh breakup regime of jets as well as during turbulent breakup at high density ratios [21, 22]. The Surface Breakup regime of jets and many of the breakup processes in sheets are similar, however. Liquid-turbulence-induced breakup mechanisms, in particular, have been shown to be similar [17, 23], clearly indicating the ability to compare the two geometries in some situations.

In terms of the third configurations, films, sheets clearly resemble them geometrically; this resemblance is not seen in comparisons of either with jets. Consequently, a greater degree of similarity is expected between sheets and films than between either, sheets or films, and jets. This section is still abbreviated, as was the jet section, but more details will be given for sheet regimes because more similarities with films are expected. The reader is directed elsewhere for more in-depth reviews, e.g. Lefebvre's [5] book on atomization or the paper by Sirignano and Mehring [24]. Similar to the abbreviation of the jet section, nonparallel (impinging) flows will not be considered here. This decision was made because 1)there is little work in the subject, 2)the mechanisms involved in nonparallel sheet atomization are found to be substantially different than those for parallel flow [3] and 3)much remains unknown for the case of parallel flow without adding this further complication.

Two different configurations are commonly encountered in sheet atomization: flat and annular (Figs. 1b and 1c). Many of the breakup phenomena are similar [25], but annular sheets have some additional complexities in the ability to impart swirl to either of the gas flows and/or the liquid flow. This swirl can change the evolution of the sheet, particularly the evolution of waves on its surface [26, 27], but the atomization regimes and general mechanisms responsible for droplet formation do not appear to change [4]. Additionally, the curvature of the sheet in the annular geometry can enhance the growth of waves on the sheet's surface [7]. As far as possible, this section is a general look at sheet atomization applying to either configuration.

A review of the literature suggests that sheet atomization can be broken down into four general regimes [4, 17, 20, 28-30]. Figure 3 presents generalized diagrams of each regime. Rarely are all four discussed within the same reference, however. The existing nomenclature for the regimes is inconsistent and confusing at times. A new classification of regimes is proposed here that is substantially more general and more related to the underlying atomization mechanisms than earlier classifications. This classification also emphasizes similarities with film and jet atomization mechanisms. Herein sheet atomization will be broken into the Sheet Pinching, Surface Breakup, Perforated and Prompt Atomization regimes. In the Sheet Pinching regime a long ligament is formed along the entire width of the leading edge of the sheet. This regime is analogous to the Rayleigh mode in jets—hydrodynamic instabilities cause the surface of the liquid to develop waves which eventually cause a part of the liquid to separate from the bulk. The Surface Breakup mode is characterized by the shedding of droplets from protuberances on the surface of the sheet and is, therefore, analogous to the same-named regime in jet atomization. While surface disturbances and sheet pinching may occur simultaneously and involve similar initiating mechanisms, they may also occur independently and are generally dealt with separately in the literature ([29], for example); consequently, they are considered to merit a

separation into two different regimes here. They may be differentiated from each other, in part, by the size of the disturbances relative to the sheet width. Disturbances in the Surface Breakup mode are smaller than those of the Sheet Pinching mode. If characteristic holes appear and induce breakup then the sheet is in the Perforated regime. Finally, the Prompt Atomization regime is like the regime of that name in jet breakup—disintegration of the sheet occurs at the exit of the nozzle [4, 6, 29]. The mechanisms involved with Prompt Atomization in sheets have received less attention than those in jets, but many parallels exist. The mechanisms causing these regimes will be further elaborated on in the Atomization Mechanisms section, but prior to that a more thorough description of the first two regimes is warranted.

Sheet Pinching is characterized by the formation of a large ligament from the entire spanwise edge of the sheet. These ligaments are either torn off the end of the sheet (due to aerodynamic forces) or form when the two interfaces of the sheet come together along a spanwise line due to surface instabilities [1, 20, 31-33] (see Figs. 3a and 3b). The large ligaments then break into smaller droplets via Rayleigh breakup ([20], for example); this secondary Rayleigh breakup would not exist in liquid films since pinching will create a ligament which is attached to the wall. This wall-bounded ligament could, however, undergo other breakup mechanisms. The Sheet Pinching regime has garnered the most attention in the sheet atomization literature and is implemented in numerous numerical calculations ([1, 20, 34], for example). A different mechanism, driven by gas pressure, is described by Adzic et al. [29] which may also cause large sections of an annular sheet to separate. These large sections undergo breakup due to aerodynamic as well as surface-tension instabilities.

The Surface Breakup regime is dominated by the shedding of droplets from disturbances on the surface of the sheet. As in jet breakup the disturbances could be waves or ligaments which are generated by liquid turbulence, hydrodynamic instabilities or other force interactions. This regime generally encompasses the rim shedding regime detailed by Chigier [6] and others, assuming the rim structures are not caused by perforations; in other words, disturbances may not exist throughout the entire sheet but only in one section such as near the exit [17, 23] or at the edges of the sheet [6, 35, 36]. Stapper et al. [35] also observe Surface Breakup at both the limits of their “cellular regime,” the main body of which falls into the Perforated regime (see also [25]), and in the “stretched streamwise ligament breakup” regime: at the lower liquid velocity limit atomization occurs from streamwise ligaments originated from a coherent sheet; at higher liquid velocities perforations appear and the sheet moves into the Perforated regime; and at even higher liquid and gas velocities the coherent sheet transitions to a series of ligaments at its downstream edge without any intermediate perforations. This example illustrates the increased generality of the four regime characterization.

C. Other Configurations

Not all configurations fit neatly into the main groupings of jet, sheet and film. Impinging jets and effervescent atomizers are two commonly encountered configurations that deny easy geometric classification. In impinging jets, the setup is initially a liquid jet but the collision of two (or more) jets forms a sheet and the subsequent breakup is from this sheet. At the exit plane of an effervescent atomizer the flow can resemble either a jet or a sheet depending on the gas-to-liquid ratio, i.e. the ratio of mass flow rate of the gas to the liquid. Impinging jet geometries are shown in Fig. 4; effervescent atomizers are illustrated in Fig. 5.

Four atomization regimes for impinging jets are reported in the literature [37-39]. All of these regimes can be related, in some way, to regimes discussed earlier. At low jet velocities the

collision initially forms a sheet but this sheet subsequently collapses into a jet [39]. Any atomization occurs from this jet, so falls into one of the atomization regimes for jets. The three remaining regimes occur at higher jet velocities and atomization occurs from a sheet. These regimes are a rim atomization regime, a periodic regime and a catastrophic breakup regime. The rim atomization regime is characterized by either periodic or random shedding from the edge of the sheet [37, 39]. This regime falls into the Surface Breakup regime, specifically a rim breakup mode, of sheets as discussed above; although, the exact details of ligament formation may differ. A periodic regime occurs when some turbulent jets collide; this regime is typified by the shedding of regularly circumferentially spaced droplets cast off from the edge of the sheet [37-39]. According to the description and diagrams given by Anderson et al. [39] and the pictures given by Jung et al. [37] this regime corresponds to the Sheet Pinching regime of sheet atomization. The cause of the waves may be different in the two geometries, however. Waves on sheets formed by impinging jets may originate due to the impact of the two jets [37], no due to hydrodynamic instabilities. The last regime, at the highest jet velocities tested, is considered to be the fully developed regime where catastrophic breakup occurs; in this regime periodic waves of droplets are shed from the point of impingement and no sheet is evident [37, 39]. In terms of impinging jets, this regime is a prompt atomization regime: droplets are formed at the earliest time possible; earlier atomization would take place from the jets before they collided. Aside from possible additional driving forces due to the impact of the two streams, the basic description of atomization regimes of impinging jets is encompassed within the discussions of jets and sheets. While impinging jets are not directly applicable to the film configuration, they are similar to the situation where a jet of liquid impacts a solid surface. The driving force unique to this configuration, impact waves, may therefore be important in some film atomization problems. Again, the above description is a drastic abridgement of this subject; for further reading the review article of Anderson et al. [39] is recommended. A similar configuration is the splash plate setup. In this geometry a jet impacts a disk of nearly the same diameter as the jet and spreads to form a sheet (Fig. 4b). This configuration is in between that of impinging jets and a jet impacting a wall. Atomization from splash plates is reviewed in two articles by Clanet and Villermaux [36, 40].

In effervescent atomizers gas is injected into the liquid at a low relative velocity in order to form a bubbly two-phase flow [41]. This two-phase flow has a much lower sound speed than either the gas or liquid alone, thus the flow in the nozzle chokes at much lower speeds. Choking creates a large pressure drop at the nozzle exit. The atomization in effervescent atomizers relies on this pressure drop [41]. Depending on the gas-to-liquid flow rate the flow in the nozzle may be bubbly, slug or annular (Fig. 5). On exiting the nozzle, the air (either the bubbles, slug or the inner column) experiences a sudden pressure drop causing it to expand rapidly [41]. This rapid expansion causes bubbles or slugs to shatter the surrounding liquid forming droplets; the annular liquid is fragmented into ligaments by this expansion [41]. These ligaments remain attached to the bulk of fluid remaining in the nozzle. Effervescent atomization will not be considered in the film regime here as no existent literature on this configuration was found; however, similar behavior could be expected with bubbles, slugs and inner cylinders—trapped air exploding the liquid in all directions except the wall-bounded one and forming attached and unattached ligaments. The behavior may also be similar to bubble rupturing events when the bubble is created by other means such as boiling. Bubble rupture is discussed in the Atomization Mechanisms section. For further review of effervescent atomization the reader is referred to the article by Sovani et al. [41].

D. Films

Much of the literature regarding film flow is focused on water waves in oceans or spillways, where atomization is not the main focus. Another large body of literature exists on heat-exchanger pipes where the focus is predicting film depths and/or heat transfer; these works are often concerned about atomization but research is centered on the entrainment rate of the liquid, not on the mechanisms by which the liquid becomes entrained. The literature that does address atomization mechanisms considers only a Surface Breakup mode where disturbances on the film surface evolve into droplets ([42-44], for example). As discussed earlier, however, there is the possibility of a regime similar to the Sheet Pinching and the Rayleigh mode where an entire downstream section of fluid separates. Perforations, though unlikely to be important factors in most rocket injectors, are also possible under some conditions [45]. Both Sheet Pinching and Perforations may result in a wall-bounded ligament, or ribbon, the breakup of which could differ substantially from the breakup of the entire film due to marked differences in shape and the existence of a liquid-solid surface tension force; therefore, these ribbons warrant further investigation. Because pinching is a misnomer in the film flow geometry and the breakup is not due to surface tension, as in the Rayleigh mode, this regime deserves a new moniker; it will be titled “Ribbon Forming” in subsequent discussions. A fourth potential regime is a Prompt Atomization regime which may exist if the liquid is initially sheltered. Potential mechanisms for Prompt Atomization of films are expected to be similar, in most respects, to those that dominate the same-named regime in jets and sheets. A quantitative examination of film atomization mechanisms will follow the more general section which qualitatively investigates the mechanisms responsible for the Surface, Ribbon Forming, Perforated and Prompt regimes. Generalized illustrations of the four regimes are given in Fig. 6.

One additional similarity and complexity shared by films and sheets bears mentioning: the existence of multiple configurations, generally flat or annular. In annular flow swirl may be added which can change the flow evolution; as discussed earlier, however, while the addition of swirl may change the growth of instabilities on the surface of the film it has not been found to alter atomization mechanisms [46]. As with the sheet and jet geometries, only flows that are, in the mean, parallel are considered here. Reasons for this abridgement include a lack of literature on the subject of atomization due to impinging air flows and the large amount of information, known and unknown, regarding the parallel configuration.

III. Atomization Mechanisms

In the Prompt Atomization regime catastrophic breakup of the liquid occurs upon exit. In all other regimes atomization occurs through the creation and, possibly, propagation of a surface disturbance followed by the creation of a droplet or droplets from the disturbance. In many regards only this last action, droplet creation, constitutes atomization. The formation and growth of the disturbance that is later broken into droplets is an important part of the entire process, however. Consequently, this section opens with a discussion of the formation of a disturbance (wave, ligament or perforation). A subsection outlining the breakdown of a disturbance into a droplet(s) follows. Again, the focus here is on mechanisms found in film atomization. Prompt Atomization mechanisms are discussed following the subsection on disturbance breakdown. This section closes with the presentation of another mechanism, film separation, which does not easily fit into the earlier sections on disturbance formation and breakdown.

A. Disturbance Formation

The disturbances discussed here include waves, ligaments, bubbles and perforations. Waves can occur over the entire surface as in the Ribbon Forming regime, or they can be localized three-dimensional structures as in the Surface Breakup regime. Ligaments are, generally, liquid projections whose lengths exceed their widths, but this term can also be used to describe any isolated three-dimensional protuberance. Bubbles may be formed by a variety of means; after formation they rise through the film, contact the interface and may rupture to form droplets. Perforations are breaks in the sheet or film, i.e. holes, which are shaped as a closed circle or oval or as an open parabola-type shape (see Fig. 6c). The main causes of wave and ligament formation discussed in the literature are liquid turbulence and hydrodynamic instabilities. Some literature also examines the interaction of gas structures with the liquid surface and pressure-driven disturbances, particularly in the annular sheet geometry. Perforation causes remain largely unproven, but work in the sheet geometry has focused on sheet thinning causing the two edges of the sheet to meet. Films may “spontaneously” form holes or holes may be induced in manners similar to those in sheets.

Liquid Turbulence

The effects of liquid turbulence on the liquid-gas interface have been studied in depth in all three geometries. Jets, annular sheets and (exterior) annular films have all been studied by Faeth and his coworkers, principally Wu, Dai and Sallam [2, 17, 22], with the findings that (in the Surface Breakup regime) the mechanisms involved did not differ appreciably between the three configurations [2, 23]. The surface mode of turbulent breakup occurs due to the interaction of turbulent eddies with the interface of the jet [14, 22, 47, 48]. This interaction causes the formation of ligaments. Sarpkaya and Merrill [48] give an in-depth description of eddy dynamics in flat films while Faeth and coworkers present a simplified, quantitative model of ligament formation [21, 22] and Mayer [47] gives detailed pictures from numerical simulations of eddies interacting with an interface.

Liquid turbulence has garnered experimental and theoretical attention in the film configuration specifically. Experimental observations by Dai et al. [2] as well as Sarpkaya and Merrill [48, 49] demonstrate that liquid turbulence leads to the formation of ligaments in film flow geometries. Dai et al. [2] compared turbulent outer annular film atomization with turbulent jet atomization and found the two to be remarkably similar allowing earlier theoretical descriptions for jets to be used to quantitatively describe the formation of ligaments on the film surface. Experiments by Sarpkaya and Merrill [48] on flat films found that any roughness on the surface of the wall disturbs the entire film and has a marked effect on ligament formation and droplet production. Their findings are based on roughness heights of 0.13 mm at a minimum in films at least 5.4 mm in depth and indicate that roughness must be accounted for to achieve accurate quantitative descriptions.

Another effect of liquid turbulence is put forward in recent work by Lioumbas et al. [50]. Their results suggest that the transition from laminar to turbulent flow may be responsible for initiating solitary waves in accelerating film flows. They define solitary waves as waves with large amplitudes and relatively long wavelengths. Their findings are for inclined, stratified pipe flows with and without parallel gas flow, but the findings are similar to those for flat, free falling films. The intermittent way in which flow transitions from laminar to turbulent is suggested as a reason for the intermittency of the solitary waves, which are separated by relatively large stretches of smooth, flat film [50]. In rocket injectors the film exists for only a short length, but

if the flow was near transition upon the film's introduction then these waves might form and play a role in atomization.

Hydrodynamic Instabilities

A large body of work on surface tension driven instabilities, particularly the Rayleigh instability, of jets exists, but, as discussed in the jet regime section, this mechanism does not directly cause breakup in films and will not be detailed here. The Rayleigh mechanism is responsible for the break down of ligaments, however, and will be further discussed in the subsection dealing with ligament breakdown. Indeed, due to the large body of work in sheets and films and the strong similarities between these latter geometries, this review will focus on the hydrodynamic instabilities of these two geometries only. Figure 6a shows one likely form of a film whose disturbances are caused by hydrodynamic instabilities

The majority of work on sheet disintegration deals with the Sheet Pinching regime and contains an instability analysis. This large body of work helps to highlight the difficulties and complexities of developing accurate descriptions of hydrodynamic instabilities. Most of the work focuses on temporal instabilities, where the growth rate is considered a function of time [51]. There is, however, a body of literature examining spatial instabilities, where the growth rate is a function of distance [51]; a limited amount of work focuses on each separately ([24], for example). Few studies address the full temporo-spatial stability due to the complexity of the resulting equations [16, 24] and continued debate exists on whether the temporal or spatial viewpoint is more appropriate [6, 16, 51]. A further complication to this debate is recent numerical studies that suggest the short-term temporal growth is important even for waves which are stable at long times [52-54]; this line of investigation shows promise because it has predicted specific three dimensional structures, streamwise ligaments [54], that classic instability analyses have had difficulties predicting [55]. An additional debate arises from the use of linearized equations to describe the instabilities. The vast majority of analyses are linear in nature due to the extreme complexity of the nonlinear formulations. Questions have been raised about the applicability of the linear theories, which must assume that disturbances are small, to the atomization process where disturbances are large [56-58]. Also, nonlinearities are, in part, responsible for the size distributions of droplets in a spray [59]. Clearly, the subject of hydrodynamic instability and instability growth on sheets is a complex and active topic worthy of its own review article; definitive conclusions on wave sizes, causes and growth rates are not yet available for the range of conditions and geometries at which atomization occurs.

As with sheet breakup, much of the literature of film dynamics describes hydrodynamic instabilities, although in this case they generally lead to Surface Breakup. Theoretical investigations into the aerodynamic instabilities of flat sheets began more than fifty years ago; seminal works in this geometry include those by Squire [57], York et al. [58], Hagerty and Shea [34], Dombrowski and Johns [31] and Li and Tankin [60], among others. Most of the instability modes of films are the same as those found in sheets, although film instability analysis has its own seminal works ([61-64], for example). Differences due to the movement of only one interface in the film versus two in the sheet play little role in the stability of the film but do effect further breakup of the liquid. Differences in boundary layer profiles between the two geometries remain important, however. Commonly considered instability driving forces include aerodynamic shear, air turbulence and/or viscous stratification. A thorough theoretical investigation by Boomkamp and Miesen [65] examines several sources in-depth and classifies instabilities in infinitely deep films. Kelvin-Helmholtz and Tollmein-Schlichting instabilities are

most often emphasized in film analyses [66, 67]. Kelvin-Helmholtz instabilities are driven by aerodynamic shear; Tollmein-Schlichting instabilities arise due to the effects of gas turbulence. It is interesting to note, although not directly relevant to the current work, that Boomkamp and Miesen [65] conclude that Kelvin-Helmholtz waves do not exist in viscous film flows—the introduction of “viscosity effects, however small, into the stability problem rules out the possibility of the essentially inviscid Kelvin-Helmholtz instability” [65]. Swirl in the gas and liquid phase of annular film flow is likely to affect film stability as it does sheet stability [26, 46], but little detailed work exists for the film geometry. As with jets and sheets, analysis of infinitely deep films has observed that velocity profiles, particularly boundary layer profiles, play an important role in determining the instability modes of a system [52, 59, 68]. In particular, gas-phase profiles, which are often neglected, have been found to be important [52, 68]. Unfortunately, exact velocity profiles are often unknown and are difficult to predict or measure. For further reading on the subject of instabilities in films the work of Boomkamp and Miesen [65], Ostrach and Koestel [69] and the notable text of Drazin and Reid [70] are recommended in addition to the seminal works listed above.

To test predictions made from hydrodynamic instability theory wavelengths can be measured from photographs of films and compared to predictions. Lavergne [71] found that the visual frequency of a sheet and the frequency of perturbations in the air speed near the sheet exit, as measured by a microphone, were in close agreement and that microphone measurements were more easily made. Even with good experimental measurements, though, assessment of theoretical agreement is complicated because it is difficult to make exact predictions due to the limited knowledge of the flow parameters in the nozzle and sheet/film; theories may require the pressure drop across the nozzle [57], the shear layer thickness [12] or other parameters not easily measured or predicted. Despite these difficulties, experimental comparisons in films have been favorable [19, 72-74].

As in sheet atomization mechanisms, film mechanisms involving hydrodynamic instabilities predict a most unstable wavelength as the one with the fastest (shortest) growth rate and suggest that this wavelength dominates and, hence, the droplet size is proportional to it [58]. This assumption has been successfully used to aid the generation of empirical correlations [73]. Despite successful comparisons, an additional complication was uncovered in a recent study by Li et al. [75]. Their numerical work showed that different droplet diameters could be generated from the same disturbances, including the same wavelength of the disturbance [75]. These findings suggest that not only wavelength, but other properties of the instability are important, for example amplitude and/or evolution time. This highlights an important point that must not be overlooked in stability analysis: the existence of an instability does not guarantee that atomization will occur. A time scale is involved for the growth of the instability; other mechanisms may produce atomization before the instability grows sufficiently to cause atomization. Finally, even a thorough description of instability formation and growth is not an atomization mechanism—a description of how the droplets form from these instabilities is also needed.

Vortices in the Gas Phase

Structures in the gas phase have the ability to displace the surface of the liquid phase provided they possess enough energy to overcome the energy of the sheet/film [9, 76-78]. A representation of this disturbance creation mechanism is given in Fig. 7. Eddies due to gas turbulence can have more indirect effects, such as changing the hydrodynamic instabilities of the

system. Compared to liquid turbulence and hydrodynamic instabilities, little atomization literature exists in which direct gas phase interactions with the coherent liquid are considered. This lack of literature may be partially due to findings by several researchers including Faeth and colleagues [21, 22] that aerodynamic effects on jets can generally be neglected, particularly if the liquid-to-gas density ratio is above 500. As discussed above, however, sheets and films are more susceptible to aerodynamic effects than jets. Also, at increased pressures, like those found in rocket engines, and the liquid-to-gas density ratio is lower and the effects of the gas phase are more important [79]. Lozano et al. [76] and Lopez-Pages et al. [78] experimentally studied the effect of gas-phase structures on the atomization of sheets; they found gas flow separation and the subsequently created vortices, which are periodically shed, helped force the flapping of the sheet. Lopez-Pages et al. [78] found that vorticity is created from the contact of the flowing gas and liquid, i.e. even with an infinitely thin separating wall vorticity is still created in the gas. The pressure fluctuations created by this vorticity are actually larger with infinitely thin walls than in the case of finite walls and this vorticity drives the flapping of the sheet even more strongly. Park et al. [72], however, found that stable recirculation zones behind separating walls actually helped to stabilize a sheet.

When considering the film geometry, no literature was found that directly investigated the effects of structures in the gas phase on atomization; there are, however, investigations of the effects of gas turbulence on the formation and growth of waves, particularly through the introduction of hydrodynamically unstable flow conditions or by increasing the growth rate of waves [19, 61, 65, 72, 80, 81]. Hydrodynamic instabilities have been addressed in the preceding section. Jurman and McCready [19] suggest that air turbulence helps cause distortions and waves on the liquid surface without giving a specific mechanism and Park et al. [72] suggest air turbulence is the source of initial perturbations which trigger hydrodynamic instabilities. Eddies in the gas may act in ways similar to liquid eddies, contacting the interface and causing deformations if they are sufficiently energetic. Any distortions can be further enhanced by the turbulent flow of air over their surface leading to disturbance growth and eventual droplet production [80, 81]. Growth may be additionally enhanced due to the nonparallel orientation of some of the velocity fluctuations [19].

Recent work includes a planned investigation of the effect of vortices created by a backward-facing step on a liquid film [82]. The single-phase work observed both stationary and shed vortices [82]. A stationary vortex might essentially constrict the flow of the film passing under it. This constriction would accelerate the flow; additionally, a thicker area of film could be created adjacent to the vortex due to the constriction. This behavior was observed in recent simulations of film flows [9]. The vortex would also change the gas flow downstream of itself leading to different aerodynamic forces. All of these would affect the subsequent behavior of the film possibly causing disturbances or their growth, but might not directly cause atomization. Vortices could produce more complex film behavior if they are strong enough to substantially distort the film surface. As an example, imagine a liquid with little surface tension in contact with a dense gas. The gas contains a clockwise-rotating vortex in a bulk flow (from left to right) as in Fig. 7. This vortex could force the film to thin in the downstream direction and drag fluid up along its upstream edge causing a wave or ligament to form. Further, if the vortex was strong enough, it could drag the fluid far enough or with enough force to separate a portion from the main flow. This mechanism may explain findings in numerical, two phase film flow simulations of “large perturbations of the gas-liquid interface with a wavelength similar in size to the scale of the large, energy containing eddies” [83]. No definitive evidence of this mechanism has yet been

reported, but the numerical results of Li et al. [75] show liquid behavior that appears consistent with such a mechanism, especially their results where the liquid and gas were the same fluid (no surface tension).

Pressure Fluctuations

Pressure fluctuations can be caused by several processes. Cavitation may drive pressure fluctuations without any interaction from the environment beyond the nozzle; Adzic et al. [29], among others [25], detailed another self-contained pressure-driven process for annular sheets which is detailed below. More often, however, pressure fluctuations are caused by changes in the environment outside of the injector, e.g. feedback from combustion instabilities [84]. These environmental instabilities may even be driven by the atomization process, creating a feedback loop that is very difficult to model. Pressure fluctuations impact atomization mainly by causing changes to the supply rate/velocity of the liquid and gas [84]. Other effects may be present, however, such as the impact waves observed on impinging jets. In general, pressure fluctuations as a means of wave/ligament creation have received less attention than the above-discussed mechanisms. Because of its importance in driving pressure fluctuations, cavitation is discussed first.

Under certain conditions cavitation can occur within the nozzle or at its exit [85-87]. Cavitation is often discussed in engine fuel-feed systems; several studies have also been done for the jet configuration. Cavitation generally occurs at the transition into the injector, but can occur at sharp corners in other areas of the injector [86]. Liquids cannot flow around sharp corners, so flow separation and strong streamline curvature results; this strong curvature generates a large pressure gradient along the flow with a low static pressure near the corner. If the pressure drops to the liquid's vapor pressure bubbles/pockets of vapor are formed. This formation of vapor bubbles is called cavitation. Cavitation generally causes disturbances indirectly, most notably by making the flow less steady and increasing the turbulence [88]. The presence of bubbles in the nozzle reduces the discharge area, causing an increase in the liquid velocity; it also enhances fluctuations in the mass flow rate either due to bubble collapse or changes in the size of the vapor pocket [86, 87]. The consequences of mass flow fluctuations are discussed in more detail below. In instances where the cavitation pockets have reached the exit plane a roughened surface has been observed immediately after the liquid exits the nozzle [87]. It is unclear if this roughness is due to an increase in liquid turbulence caused by the cavitation, a result of the greater time the liquid is in contact with gas or due to some other interaction of the vapor and liquid—the cause of the surface disturbances are unclear but are clearly effected by the cavitation [87, 88]. Asymmetric cavitation has been observed in jet-producing nozzles with asymmetric inlets where it was found that this cavitation region is more unstable than in symmetric jet nozzles [86]. Since films have a free surface any cavitation which occurs within the film will be asymmetric. The instability of the cavitation region results in strong pressure waves being sent through the fluid when the bubble collapses [86]. As mentioned above, pressure waves can affect mass flow rates; in films, where one side of the liquid is constrained, they may also cause surface waves regardless of changes in flow rates. This wave production mechanism would be similar to the development of waves at a beach where the amplitude of the wave energy is larger than the film depth.

Pressure fluctuations can cause an uneven feed velocity/mass flow for the fuel or gas. If these mass-flow changes are large enough they can create a change in liquid thickness, e.g. a “bulge” of liquid following a dip in gas pressure. These bulges would likely appear as singular

waves with relatively flat interfaces preceding and following them. Experimental studies have shown that pulses of fluid in an annular film configuration can lead to atomization of an otherwise nonatomizing flow [44]. Additionally, changes in fuel and gas velocity alter many of the fundamental characteristics of the flow. These changes lead, in turn, to differences in hydrodynamic stability behavior, wave growth, aerodynamic shear, etc. [84]. When the fuel and gas velocity are affected by pressure changes the growth and breakdown of disturbances will be altered.

In the case of impinging jets, pressure fluctuations in the jets may lead to impact waves. These waves, instead of waves produced by hydrodynamic instabilities, may be responsible for atomization [37, 39]. The waves are generated by pressure or momentum fluxes in either or both jets; they may also be present in a film configuration if the film is formed by a jet impinging on a wall. These fluctuations may be generated inside the nozzle producing the original jet by the instabilities of the jets prior to impact, due to cavitation in the jet nozzles or due to turbulence within the jet [39]. The velocity profile of the jet also affects impact waves. When the jets are laminar, the boundary layer helps to damp the waves, but the flat profile of turbulent jets does not contribute to damping the waves [37]; consequently, impact waves are more prevalent in the impingement of turbulent jets. Predictions based on theories of impact waves compare favorably with experimental results for the collision of two jets, especially when comparing the differences in the impingement of laminar and turbulent jets [39]. Available literature on atomizers that utilize jets impinging with walls do not report these impact waves, however [74].

Another effect of pressure is found for annular sheets. The experimental work of Adzic et al. [29], for example, describes several different subregimes in what is here termed the Sheet Pinching regime (their “Kelvin-Helmholtz” regime). These subregimes are driven by pressure changes in the interior hollow of the sheet [29]. At low inner-air velocities the sheet forms a hollow bulb shape. The cylindrical sheet comes together at the downstream creating a closed shape; the interior air is trapped and the additional air fed to the system increases the pressure inside this “bubble”. Eventually the pressure and surface tension forces cause the upstream inlet of the bubble to neck down and seal, often separating a large section of liquid from the upstream mass of the sheet. Liquid instabilities further downstream cause the bubbles to burst. If both inner and outer gas flows are present, the bubble can be quite distorted and, consequently, burst before it is closed [29]. This bubble-forming behavior cannot directly occur in film flow, but an imperfect comparison can be made with flows that change from slug (or near slug) flow to annular flow, where gas flow may be constricted downstream leading to a cyclic buildup of pressure. It, therefore, seems worth noting that in sheets, and potentially in films, fluctuations in air pressure can be important, even if they are assumed not to affect the liquid feed.

Bubble Formation

Gas bubbles can be formed in the film due to the entrainment of air, by a gas coming out of solution or by vapor bubble formation (cavitation or boiling). Gas can also become trapped in the film by a variety of mechanisms which are generally due to the breakdown of other disturbances. Several authors discuss gas entrainment due to breaking waves [89-91]. Both spilling and plunging breakers, described in the wave breakdown section, entrain air and create large numbers of bubbles in the volume near the breaking event. However, the findings seem to indicate that smaller waves produce fewer bubbles [90, 91]; most studies are of waves on the scale of those found in oceans not those found in atomizers. The collision of a droplet or collapsing ligament with the film may also entrain air [92]. Again, small amounts of air and,

consequently, few bubbles are produced in these events. Woodmansee and Hanratty [93] mention air entrainment due to an interaction of ligaments and waves, perhaps via ligament collapse. There is also the possibility that gas-phase turbulence could cause deformations of the interface and lead to air being entrained in a manner similar to the way in which ligaments may be created from liquid turbulence.

Lefebvre [5] discusses taking advantage of dissolved gases and/or boiling in a section on effervescent atomization, a term which is now used differently. In today's common usage effervescent atomization involves gas being purposely introduced into the liquid as discussed above. If the gas is purposely introduced into the flow and the flow is not choked at the injector nozzle, bubbly flow will result. There may be a change in pressure or temperature along the film which could cause dissolved gases to come out of solution forming bubbles. A hot wall could cause the liquid to boil producing vapor bubbles. Also, cavitation in the nozzle could introduce pockets of vapor into the liquid (see the Pressure Fluctuations subsection above) although these likely collapse quickly. Once gas or vapor bubbles are formed in the film they rise and may interact with the gas-liquid interface likely leading to some droplet production (see Fig. 13).

Perforation Causes

Perforations are a different type of disturbance that leads to atomization. Atomization due to perforations occurs at the upper limit of the “cellular regime” of atomizing sheets described by Stapper et al. [35]. They observe in their experiments that perforations arise due to localized thinning of the sheet in the streamwise direction as a reaction to streamwise vortices. A limited amount of work exists on this mechanism, but other explanations have been offered as causes for perforations. Fraser [28] observes sheet perforations under certain conditions and suggests that solid particles in the liquid, gas release in the form of bubbles within the sheet, droplet impingement or ripples may cause perforations. Fraser [28] tries various experiments to elucidate the mechanism(s) involved and concludes that bubble release and droplet impingement are unlikely. No concrete information was found supporting any specific mechanism; however, ripples are seen in all cases where perforations form. Indeed, even more than forty years later the author found no definitive experimental evidence as to the validity of these potential causes. Hydrodynamic instabilities have also been pegged as a possible cause of sheet perforations [38, 58] and may be responsible for the ripples observed by Fraser [28].

These suggested mechanisms are possible in the film configuration; however, no literature was found that deals with atomization due to film perforations. Indeed, film perforations are less catastrophic than sheet perforations because the wetting of the wall creates a surface tension force opposing the growth of the hole. Films may be more likely to develop holes, however, as they have additional perforation causes. Film flows may “spontaneously” rupture or dewet due to surface imperfections or forces on a molecular level. Circumstances that lead to perforations and streamwise ligaments in sheet flows may cause streamwise ribbons to form in a film as well. The film may even be split down to the wall producing a series of ribbons or rivulets, especially in a liquid where the restoring force to close a break and rewet the surface is small. Additionally, a commonly observed ribbon-forming phenomenon is the splitting of a film as it flows down an inclined or vertical wall. In this situation the ribbons are called rivulets. Rivulet formation and stability is important in cooling towers where a break in the film can cause hot spots and failures [45]. Many theories and correlations have been developed to predict the stability and formation of ribbons on inclined surfaces [45, 94]; the gas and liquid flow rates are generally considered to be very small in these theories. Ribbon formation has also been

observed on the surface of rotating cups and disks and a theory exists to calculate their formation [95]. This mechanism remains largely unexplored in atomization literature, despite its possible importance for flows of metal and polymer melts where the liquid-solid surface tension may be small. Perforations are unlikely to dominate the behavior in most film atomization operations until the later stages when the film has thinned substantially. It is likely that by this point the bulk of the atomization properties will have been defined by the previous breakup of the bulk of the film. Perforations may be important, however, if the film is initially thin or if the liquid barely wets the injector material.

B. Disturbance Breakdown

In order for atomization to occur a disturbance must evolve into a droplet. Again, the reader is reminded that the breakdown process requires a finite time and a minimum disturbance height, so that not all disturbed surfaces will undergo atomization. Descriptions of disturbance formation, therefore, are an important part of, but do not fully describe, atomization mechanisms. The following discussion is partitioned based on the type of disturbance creating the droplet(s): wave, ligament, “particle” (i.e. bubble or droplet) or perforation. For the purposes of the following discussion a wave is a protrusion that is generally wide and always wider than it is high; contrarily, a ligament is a protuberance that is generally long and always longer than it is wide. There is some overlap of breakdown mechanisms between these two disturbance types.

Wave Breakdown

As discussed above, various mechanisms may produce waves. These waves may stay the same height; shrink due to energy losses, such as viscous diffusion; or grow due to aerodynamic enhancement (lower pressure over the wave due to flow acceleration over a curved surface), the overtaking of one wave by another or additional wave producing events/drivers. Many papers focus on the growth of waves through aerodynamic enhancement ([6, 76], for example) and studies have shown wave coalescence to be important [96, 97]. Several wave breakdown possibilities exist: liquid may be stripped from the crests of waves; growing waves may break, like waves on a beach; waves may split to produce a series of ligaments (similar to a rim disintegration mode) or form a large three dimensional disturbance that would qualify here as a ligament (in other words, change classifications); or waves may cause a long ligament of liquid to be cut-off from its surrounding fluid, i.e. Form a Ribbon. Ribbon formation changes the physics of the flow and may be indirectly responsible for droplet formation. Stripping occurs in both waves and ligaments, but is dealt with in the Ligament Breakdown section below.

The existence of complex three-dimensional gas and/or liquid disruptions, such as observed by Stapper et al. [35] can cause single waves or the edge of the sheet to split into multiple waves or ligaments. As the wave grows the streamwise disturbances cause thinning in some areas. Eventually these thin areas within the wave rupture creating multiple waves/ligaments [35]. Other perforation causes may act locally on a wave to produce the same results, especially if the wave is steep. Waves may become ligaments attached to the main flow in ways other than splitting. An example is found in the numerical experiments by Li et al. [75]. In this study a hypothetical two-dimensional fluid with no surface tension shows wave growth through the interaction of a vorticity with the surface. While this experiment shows growth along the entire wave, it is possible that local vortices could cause local growth of an area on the wave until its height exceeded its width. Coalescence of three-dimensional waves may also cause a wave to increase in amplitude until it is higher than is it wide. Once a wave has evolved

to this extent other mechanisms, as discussed in the ligament breakup section below, may cause droplets to be produced.

The formation of a long ligament from a wavy sheet or film occurs in the Sheet Pinching and Ribbon Forming regimes as discussed above. This mechanism is the most commonly considered one in sheet atomization. The ribbon can be formed when a long section of liquid is torn from the sheet [31] or by the meeting of the troughs of waves on each interface (sheets) [1] or the meeting of the trough with the wall (films). Most works, both early and recent, which deal with sheet atomization due to hydrodynamic instability growth, assume the tearing mechanism causes a ligament to form at half wavelengths [1, 20, 31, 98]. In sheets, once this large ligament is formed, it is assumed to undergo breakup according to Rayleigh's analysis [20, 31]. In films a wall-bounded ribbon would be created instead of a free one. Because this ribbon of fluid wets the surface, breakup via the Rayleigh mechanism would not occur. However, the curved shape of the ribbon would introduce strong aerodynamic forces and might cause a section of the ribbon to detach from the wall. In a more wetting fluid, i.e. one with greater surface tension forces, this additional aerodynamic force would likely change the shape of the ribbon only, creating a higher, narrower segment (see Fig. 10). This segment might undergo wave breaking, stripping or splitting into ligaments or remain coherent. Experimental support for ribbon forming was not found in atomizer literature, however.

Growing waves may reach a size where they are no longer self-supporting. Wave growth is generally caused by aerodynamic enhancement or wave-wave interaction [89] but could also be caused by changes in the wall geometry. Waves that are no longer self-sustaining will break, as waves do on a beach. Two main types of breaking waves exist: spilling and plunging. Spilling breakers occur in the small wavelength waves (<2mm) expected in atomizers and are characterized by a capillary-gravity "bulge" on the front-side of the wave which, eventually, leads to turbulence on the downstream/leeward side of the wave [99]. This turbulence could generate additional disturbances through turbulent-liquid mechanisms, but does not produce droplets itself. Plunging breakers create a jet which plunges into the film ahead of the wave [99]. This type of breaking is more energetic than spilling and droplets are created from the interaction of the jet with the film, similar in many ways to splashing during droplet impact [89]. Figure 9 illustrates the two types of waves just prior to breaking. Studies of turbulent liquid films [48] have observed ligament collapse producing droplets in a mechanism similar to the jet collapse in plunging breakers [92]. Both studies of turbulent film jet collapse and breaking waves conclude that this mechanism creates only a small number of relatively small droplets. Indeed, numerical models from the literature suggest that each plunging breaker would produce a very limited number of droplets [89]. Both types of breaking entrain air which may lead to atomization through bubble collapse [89, 92, 99]; still, bubble rupture creates a fine spray and a few larger droplets, so many bubbles would be required to burst before appreciable atomization would occur. Both splashing and bubble rupture are discussed later. All of these findings suggest that wave breaking is of secondary importance in atomizers. This viewpoint is furthered by suggestions from wave stripping theories that few waves would progress to breaking conditions because of mass loss due to stripping.

In a mechanism that, in part, resembles wave breaking [89], the wave may be undercut due to liquid or gas eddies at its base. This undercutting causes the wave to fall in a manner that resembles wave breaking but occurs with less speed and a smaller mass of liquid. Consequently, an open air pocket can be formed between the wave and the surface. The motion of the film entrains air into the pocket, causing it to grow. Eventually, the air pressure inside this "bag"

causes the liquid forming the pocket to catastrophically fail producing small droplets and a thick rim at the pocket's upstream edge. This rim then devolves to droplets via the Rayleigh mechanism. This process is one of the few that has been experimentally observed for film flow and is shown schematically in Fig. 10; Azzopardi [44] reports observing it in a study of annular, vertically upward film flow. Parallels can be drawn between this process and “bag” breakup of droplets [44]. Woodmansee and Hanratty [93] study atomization in a somewhat similar mode. In their experiments they observed a secondary wave accelerating and partially separating from the film to form a thick ligament. This ligament was stretched and thinned by the air flow until it ruptured. Due to their under-film imaging technique and the relatively thin nature of the bag there is a possibility that the ligaments observed by Woodmansee and Hanratty [93] had attached thin films and that their results indicate bag breakup for flat films as well as the bag breakup observed by Azzopardi [44] for annular films. Unfortunately, no further description or evidence of this mechanism was found in the literature.

Ligament Breakdown

Numerous mechanisms can cause ligaments to evolve into droplets. These mechanisms include stripping which also occurs in waves. Droplets can also be formed by the Rayleigh mechanism or when liquid turbulence cuts ligaments off at their base. Another, less explored, possibility parallels the idea of the fragile shattering of droplets described by Khavkin [100] where viscous droplets subjected to deforming forces behave as solids. Finally, ligaments may collapse due to their weight or the aerodynamic forces on them; these collapses may cause splashing as discussed in the “particle” interaction subsection. These breakdown modes are roughly illustrated in Figs. 11 and 12.

Ligament/wave stripping is one of the most commonly considered types of droplet formation from a film. In this mechanism, the gas strips a mass of liquid from the tip of a wave or ligament once it has reached a particular size [69, 93, 101]. The quantitative application of this mechanism is hindered by a number of factors, but comparisons of semi-analytic derivations with experimental results show promise [10, 43, 69]. Uncertainties in application are rife and arise from a lack of knowledge and predictive capability, for example the distribution of wave/ligament sizes and their relative velocities are rarely known. A main uncertainty is knowing when, i.e., at what disturbance height, and how much liquid is sheared from the film. Holowach et al. [43] suggest that the maximum amount of lost liquid occurs when the forces on the distorted wave tip are evenly balanced; Mayer [101] assumes waves break off when the amplitude of the wave equals its wavelength; Woodmansee and Hanratty [93] observed that secondary waves separate from the main wave due to variations in air pressure induced by the flow over the waves. In reality, there is some probability that a protuberance will lose mass to stripping, one that increases with amplitude and relative velocity between the liquid projection and the gas. Also, there is some range of mass that can be sheared from the projection. Because of this range of possibilities, analyses like Holowach et al.’s [43] that look for a maximum are appealing. An additional uncertainty in these formulations relates to disturbance shape, particularly wave crest shape, which affects the aerodynamic forces on the liquid. Azzopardi [44] reports what appears to be experimental evidence of this type of atomization in annular flow. A very large percentage of the ligament is lost, however, so the liquid turbulence mechanism of the paragraph after next cannot be ruled out based on the limited amount of information available.

The Rayleigh mechanism for droplet creation from ligaments is the same as that responsible for the breakup of low speed jets. Instabilities driven by surface tension cause the oscillation of the ligament surface and, eventually, the creation of a droplet [5]. This mechanism has been observed and described by several investigators studying atomization due to liquid turbulence [2, 21, 48]. Rayleigh's theory predicts the creation of droplet 1.89 times the diameter of the jet [5]; experimental observations indicate that droplets created during turbulent liquid film flow are slightly smaller, but on the same order as these predictions [48].

The experimental studies of Sarpkaya [49] dealing with film atomization due to liquid turbulence found that some ligaments detach from the film at their base. He hypothesized that turbulent eddies at the base of these ligaments cause them to separate from the fluid. This study and others, also in air-water systems, investigating turbulent-liquid flow showed that most ligaments break up due to the Rayleigh mechanism, but that some undergo this turbulent separation [2, 49]; both sets of experimenters estimate that 90% of ligaments undergo Rayleigh breakup and 10% undergo separation due to eddy interaction. For different liquid-gas combinations this percentage may change. The droplets produced by this method are much larger than those created by the Rayleigh breakup mechanism because they contain the entire volume of the ligament. If the size (and, hence, volume) of the ligament is known, the size of the resulting droplet can be calculated. No prediction of when and where this turbulent separation will occur can be given, but the location and frequency of shedding may be dealt with in a stochastic manner.

Fragile shattering occurs when the liquid is unable to react (by deforming) to its surrounding unsteady flow because the required speed of deformation exceeds the speed of liquid molecule relaxation [100, 102]. Because the fluid is unable to relax quickly enough it acts, essentially, as a solid. Khavkin's [100] theoretical examination of secondary droplet breakup concerned flow in pressure swirl atomizers where the droplets were subjected to uneven force loading due to the centripetal forces, which acted to deform the droplets. If the viscosity of the liquid is sufficiently large it delays this relaxation; consequently, the liquid reacts like a solid and shatters. Ligaments subjected to swirl or other velocity fields that vary along their lengths could also undergo shattering if their viscosity and the forces acting on them were large enough. At this time, however, the existence of this mechanism in ligaments remains speculation. It has, however, been observed in secondary droplet atomization in accelerating flow fields [102].

“Particle” Interaction

Discrete objects may interact with the interface of the film. Two types of objects are considered here: bubbles and droplets. Bubble creation was considered above while this entire paper is focused on droplet formation. Bubbles rising to the surface and bursting have been studied for atomization in quiescent and slow moving films such as oceanic flows. Droplet impingement on walls and films has received a lot of attention in terms of heat transfer and the removal of droplets from the gas, but less in terms of atomization. Exploration of the literature suggests that neither mechanism will be of primary importance when the goal is to fully atomize the film. Still, droplet collision and bubble rupture can create droplets and contribute to the spray characteristics. Not considered here, but of importance in special cases, is the possibility of solid particles interacting with the surface. Solid particulates could cause splashing as droplets do or they could alter the properties of the liquid through surface contamination.

After a bubble is created it rises through the fluid. Since films generally require an acceleration gradient in the direction from the interface to the wall to remain attached to the wall,

these rising bubbles will contact the interface and interact with it. Droplets and projections are created through the bursting of these bubbles as shown in Fig. 13. Two types of droplets can be created [103-105]. Film drops are created by the bursting of the thin film formed between the top of the bubble and the gas. Film droplets are very small, on the order of a few microns [103, 105]. The second type of droplets, jet drops, form from jets created by the collapse of the bubble cavity. Jet droplets are tens to hundreds of microns in diameter [103, 105]. Not all of the jets created by bubble rupture result in the formation of droplets; bubbles must be below a critical size for their collapse to produce a jet that devolves into one or more droplets [104]. “Jet” is the typical nomenclature for this disturbance, but in the context of this paper it would more correctly be called a ligament.

The process of jet formation has been studied experimentally ([106], for instance) and numerically [103, 105]. Good agreement exists between the two types of studies. Jet production proceeds through the following stages. First the bubble cap ruptures leaving a cavity in the surface of the film. A series of capillary waves are formed which converge to the base of the cavity. This convergence may trap small, compared with the initial bubble size, air bubbles. The interaction of these waves generates a ligament in the center of the original cavity. The ligament then breaks down into one or more droplets [103, 105]. Generally the ligament is assumed to break down due to Rayleigh instabilities, but it could, in principle, be fragmented by the other ligament breakdown processes. Also, as stated above, it may collapse back into the film without creating any droplets. The results of the above-cited studies suggest that, when atomization of the entire film is the goal, droplet production due to bubble rupture is not of primary importance.

The collision of droplets with a liquid film is an entire subject of its own. Studies centering on atomizing flows are rather limited, with consideration generally given to the impact of a single droplet with a film where the creation of the initial colliding droplet and the behavior of ejected droplets are given little or no consideration. This lack of focus on atomizing flows may be the result of earlier findings by Woodmansee and Hanratty [93] that splashing was of lesser importance than other droplet creation mechanisms when considering atomization. More likely, however, it is a result of the complexities and on-going evolution of knowledge of single droplet collisions with films. When a droplet collides with a liquid interface it may bounce, merge or create secondary droplets [107]. Secondary droplet creation takes one of three main forms: partial absorption, corona splash or prompt splash [107, 108]. These three modes are presented in Fig. 14. Partial absorption occurs when the droplet initially merges with the film, but a single, wide projection is subsequently created. This protuberance leads to the creation of a single droplet [107]. Corona or crown splashing is the type which often appears in photographs. In this type of splashing a thin liquid sheet is created shortly after the droplet impacts the surface. This sheet spreads radially outward and generally develops into fingers which break due to Rayleigh instabilities [108]. Single jets and corona sheets do not necessarily break up into droplets. The last type of secondary droplet creation is prompt splash which, like prompt atomization, takes place immediately after impact without any observable sheet or jet [108]. The value of the Reynolds and Weber number of the colliding droplet determine whether a secondary droplet is created and which form the creation takes; as Reynolds and Weber numbers increase the collision result changes from absorption (no droplet creation) to partial absorption to corona splashing to prompt splashing [107, 108]. Throughout the remainder of this paper, the creation of secondary droplets as a result of the collision of an initial droplet with the film will simply be referred to as splashing.

Splashing can also occur when liquid projections, such as ligaments, collapse. Studies of ligament collapse during the atomization of turbulent liquid films have revealed that, in this configuration, splashing creates only a few very small droplets; additionally, ligament collapse appears to be less common than ligament breakup [48, 92]. Indeed, splashing is unlikely to be an important droplet creation mechanism in atomizers where the goal is the transformation of the entire film to droplets. For splashing to be important in atomizers a large percentage of the atomized mass would have to come from impacts. Droplets created by splashing impacts will be smaller than the impinging droplet [107, 109], so this condition would require the bulk of the initially created droplets to impact the film. Additionally, atomization through splashing cannot be self-sustaining—eventually droplets will be created that are too small (and/or too slow) to produce new droplets. Smaller and slower droplets are less likely to splash for multiple reasons. First, splashing only occurs at sufficiently large values of Reynolds and Weber numbers [107, 108]. Secondly, in order to impact the film droplets must have enough momentum to follow a path different than the streamlines of the gas flow which are here considered largely parallel to the interface. Another reason splashing is unlikely to be important in atomizers is that the film exists for a relatively short distance limiting the number of collision events. In situations where atomization is not the primary goal, such as in cooling tubes, the film may be intact over a larger length increasing the importance of splashing. The overall lower number of droplets and a greater likelihood for secondary droplet dynamics (such as coalescence) may also increase the importance of droplet creation due to splashing in situations other than atomizers.

Perforation Evolution

Numerous works mention or deal exclusively with atomization due to perforations in the sheet geometry ([28, 35], for example). The growth of holes in quiescent polymer films occupies the bulk of literature on perforated films; in these systems the “droplets” formed are attached to the bounding wall [110, 111]. A large body of literature also exists on the formation of rivulets in vertical and inclined film flows [45, 94, 112]. Holes in sheets rapidly grow larger due to surface tension forces; holes in films may grow, shrink or stabilize [112, 113]. Only stable or expanding holes are of interest here. A thick rim is formed around an expanding hole [28, 113]. This change in topology may be important and is likely instrumental in any further evolution into droplets. Holes in flowing films take on parabolic-like shapes with thickened rims [94, 114]. The rim surface is curved above the surface of the bulk film and the flow will, consequently, be over a curved surface. This accelerated flow may separate part of the rim from the wall or bulk film as may occur in flow over ribbons. This separation may result in bag breakup if a thin liquid sheet remains attached to the wall or in Rayleigh breakup of a separated ligament.

In sheets two modes of droplet creation due to hole growth exist: droplets can be produced by the collisions of the raised rims surrounding the holes or from the breakdown of the network of ligaments which are created by multiple holes [28]. Air-borne droplets may be created from the collision of rims in a film as well, but this mechanism has not been reported in the literature. Possibly, the smaller growth rate of film perforations results in collisions with insufficient force to generate droplets. Rim collision may produce droplets by several modes analogous to those discussed above. At slow speeds they may behave like coalescing waves. This would lead to a temporary increase in the rim’s size which may increase the likelihood of wave breaking, stripping or bag breakup. If the rims collide with more energy the result could resemble splashing. The behavior could resemble a large ligament collapsing as a smaller width rim collided with a wider one or the energy of the collision could produce a tall, narrow

disturbance which subsequently separated into ligaments (fingers) and then into droplets. To date nothing of this nature has been observed; indeed, the author found no description in the literature of the mechanism by which the collision of rims produces droplets in sheet perforations. Multiple perforations could create a network or thick ribbons which would alter the atomization of the film. The generation of the large number of holes needed for this result is not expected in most atomization processes; at least not until the film becomes quite thin. Still, the formation of even a single hole or rivulet could be important because the gas flow over the film would be altered and this could change the inception and evolution of surface disturbances.

C. Prompt Atomization Mechanisms

The mechanisms considered here are those that produce immediate disintegration upon the liquid's exit from a injector. This regime might occur in a film configuration where the liquid was initially entirely contained. Reitz and Bracco [15] note the possibility that there is still some (undetectably small) intact length of the jet and that atomization, therefore, is not truly instantaneous. This assertion helps explain many of their results but verification is, obviously, quite difficult. Jet breakup in this regime has been variously attributed to cavitation, liquid turbulence, velocity profile relaxation, acceleration in the boundary layers, pressure fluctuations and aerodynamic effects, although experimental findings concluded that no single mechanism can explain the entire regime [15]. Less work seems to exist on the Prompt Atomization regime of sheets compared with that of jets. A few potential arguments for additional, sheet-related mechanisms can be gathered from the literature.

Velocity profile relaxation causes atomization due to the perpendicular velocities which may be already present in the liquid or may be caused by the liquid's change from confinement to free. This relaxation is likely to be less disruptive in a film arrangement due to the existence of only one free surface. Boundary layer relaxation/acceleration causes disintegration due to the changes in tangential stress at the interface and *instabilities* associated with the sudden change in boundary conditions. Studies show that the boundary layer profile affects instabilities on the surface of jets and films [115, 116]; this effect could clearly be important if there is any intact film where the disturbance creation would then be described by hydrodynamic instability growth discussed above. Boundary layer changes, like velocity profile relaxation, are less likely to be catastrophic in films than in sheets. Neither of these profile mechanisms has been proven, however.

Cavitation, liquid turbulence, pressure fluctuations and aerodynamics effects are known to have an effect on intact lengths of jets or sheets and have been dealt with in prior sections. Aerodynamic effects lead to the sheet behavior and shortening discussed in the previous paragraph, but a short intact length of fluid must be present for instabilities to have the time/distance to grow and cause atomization. Cavitation causes pressure disruptions that may increase turbulence and help to disintegrate the liquid. Turbulent flow contains a radial component which may cause atomization. Ghafourian et al. [38] give more information about the effect of pressure fluctuations on prompt atomization. Again, in Reitz and Bracco's [15] study of jet atomization, no single one of these were found to be the cause of all atomization behavior, but cavitation and aerodynamic effects help to explain a large part of jet behavior in the Prompt Atomization regime. The conclusions in that work strongly imply that some intact jet exists at the exit moving Prompt Atomization into the Surface regime discussed above.

Some additional, although less detailed, explanations are suggested in sheet literature. Work by Khavkin [30, 117] relates the droplet size produced in the Prompt Atomization regime

back to the Kolmogorov length scale for turbulence. Khavkin [30, 117] explains his idea through a comparison with the breakdown of turbulent structures where intensive mixing inside the atomizer is equivalent to turbulent diffusion with particles changing their size and location instead of vortices. Particles divide until they reach a stable size determined by viscosity, i.e. the Kolmogorov length scale. A theoretical description of resultant droplet sizes is formulated, but exact details on the formation of the particles are not given [30, 117]. His studies involve the behavior of pressure swirl atomizers where contact between the two phases may occur prior to the exit; in other words, atomization may not be prompt but instead may occur from the film prior to the liquid exiting the injector. Indeed, recent studies [9, 10, 83] observed a large amount of atomization occurring within their unique atomizer, in a location where the fluid is a film. This internal breakup mode means there is little or no intact sheet at the exit, but it can only occur if the liquid and gas are in contact prior to exiting the injector. Despite appearances, this breakup is not truly Prompt Atomization because film atomization occurs prior to the injector exit and should not be discounted. Unfortunately, due to the difficulty in studying this Prompt Atomization regime, the preceding list of potential causes is likely not exhaustive but instead a sampling of the commonly discussed possibilities. Taken as a whole, however, the literature suggests that from the current perspective of elucidating atomization mechanism Prompt Atomization may not exist. Instead, a small intact length of the film may always exist on which disturbances are rapidly created and broken down into droplets.

D. Film Separation

A final mechanism, which is unique to films, is separation around a corner. As a film flows (or tries to flow) around a corner there is an adverse acceleration relative to the density stratification. This acceleration can cause the film to separate from the wall. When this happens atomization can occur through two mechanisms. Either the separation causes a ligament or droplet to form at the corner, similar to a Sheet Pinching mechanism, or the film separates from the wall becoming a sheet and breaking up from the sheet geometry (see Fig. 15). Maroteaux et al. [118] looked at the possibility that the adverse pressure gradient causes Rayleigh-Taylor instabilities at the corner and postulated breakup at the corner if instabilities are above an empirical value. If the wave is larger than this value then a ligament will separate from the corner along the trough of the wave creating a long ligament [118]. This breakup is then exactly analogous to a Sheet Pinching/Ribbon Forming regime. If the instabilities are not as large, the film may depart from the wall but remain intact for some distance. In this case the liquid will behave as a sheet for atomization processes and its actual breakup is beyond the scope of this paper. Recent experiments [119] do not show Sheet Pinching at the corner, but do find an additional outcome where part of the film separates into a sheet and part remains attached to the wall. Some prediction of the conditions under which this separation occurs will be discussed in Section IV.

IV. Quantitative Descriptions of Film Atomization

Now that a general understanding of various film atomization mechanisms has been established this knowledge can, ideally, be used to predict the characteristics of the resultant spray. In order to fully quantify the spray, however, the flow field of the gas and liquid often must be completely known. This level of knowledge is not currently available for most systems and, although the capability of predicting these fields through numerical simulations is improving, the complexity of atomizing flows makes attaining and processing such information

difficult. The results of experimental investigations help to navigate the gaps in knowledge and lead to important nondimensional groupings and empirical correlations. Additionally, simplified theories have been developed for some mechanisms which lessen the need for difficult-to-obtain information. This section begins with a general presentation of important nondimensional groups in film atomization. Theories related to specific atomization mechanisms and submechanisms are presented next. The section closes with a brief presentation of empirical correlations available in the literature, particularly for the onset of atomization, entrainment rates and film thicknesses.

A. Dimensionless Numbers

In order to fully describe a flowing air-liquid system the following parameters are required: velocity, density and viscosity of the gas and liquid, thickness of the liquid layer and surface tension. Information about turbulence generation may also be necessary. If the gas layer is not semi-infinite its thickness must be given as well. Theories may also require a knowledge of the boundary layer thickness and velocity profile of both fluids. Root-mean-square velocity fluctuations, disturbance wavelength, average disturbance height, wall roughness and/or wetting angle may be important in describing the flow. Finally, accelerations, if present, must be known so that, in cases with inclination the angle of inclination will be important.

In rocket injectors and other processes where fine atomization is desired, the driving forces are likely to be aerodynamic, viscous and surface forces with gravity's contribution being negligible. In other systems, such as nuclear cooling tubes, gravity is often important but aerodynamic or viscous forces may be negligible. It should also be noted that acceleration forces, for example due to swirling flows, may be important regardless of the importance of gravitation acceleration. A review of the literature shows nondimensional groupings commonly used to account for the effects of various forces. Typically Reynolds number(s) and/or the viscosity ratio are used to describe viscous forces. Surface force contributions are usually portrayed through a Weber number. Gravity or acceleration forces are often represented by a Froude number, Archimedes number or Bond number; a nondimensional disturbance height parameter may also be used to supplement or replace the force ratio. Density ratios and/or some relation between the liquid and gas velocities frequently appear to depict aerodynamic effects. The relation between the velocities could be a simple ratio of velocities, the momentum flux ratio (or, equivalently in many cases, the kinetic energy ratio of the phases), the ratio of volumetric flow rates (also commonly called the air-to-liquid ratio) or the momentum ratio. The commonality of these various groupings can be seen in Table 1 which reviews the nondimensional parameters used in some of the papers cited within this manuscript.

Further insight may be gained by examining the important forces and information that is needed to capture many of the creation and breakdown mechanisms presented above. Many of the mechanisms require a knowledge of the turbulence levels or some information about the boundary layer(s). To scale these parameters requires matching Reynolds number [120]. As mentioned above Reynolds numbers also quantify viscosity forces; a Reynolds number is needed for each phase. Many of the breakdown mechanisms involve comparing the surface forces to aerodynamic forces. The ratio of these can be represented through a Weber number based on gas properties [121]. If aerodynamic forces are of lesser importance then the Weber number would be based on liquid properties; alternatively, in the rare atomization case where viscous forces were negligible, a Capillary number could be used. Wave growth, ligament collapse, splashing, bubble rupture and wave breaking are all dependent on the acceleration field. Acceleration

effects, including centripetal accelerations, for these events seem best captured through a Froude number where acceleration is used generically instead of gravity (aL/v^2). Froude number is chosen over Archimedes (or Ekman number for swirling flows) because the inertia of the disturbance is generally what is being counteracted not the viscous forces of the liquid within the disturbance; accordingly, the length used in the Froude number should most correctly be a characteristic size of the disturbance. In surface-tension dominated flows the Bond number may be more applicable than the Froude number. Finally, the relative forces between the gas and liquid or, more accurately, the energy difference between the two must be represented. Momentum flux ratio is often used to capture this difference when studying jets [47] and sheets [1, 68, 76]. This ratio seems like a good choice because it is essentially equivalent to the kinetic energy ratio between the two phases, and the energy between the phases dictates how much of an effect each phase is able to exert on the other. The ratio of momentums does not seem justified as illustrated through a simple thought exercise considering the case of a semi-infinite gas. The momentum of this gas is $\rho_g v_g^2 A$; if the gas is semi-infinite then the area is infinite and, consequently, the momentum is infinite as long as the velocity is nonzero. So, then, for many applications the collection of important nondimensional numbers will include a liquid and gas Reynolds number, a gas-based Weber number (alternately Capillary number), a Froude number (alternately Archimedes or Bond number) and the kinetic energy ratio of the phases.

This selection is a total of five groupings. As mentioned above, for typical applications there will be nine important parameters: the velocity, density, viscosity and thickness of both fluids and the surface tension. Buckingham- Π theory, then, necessitates six dimensionless groupings to fully capture the flow parameters (9 parameters – 3 native units = 6 groupings). Traditional application of the theory would suggest groupings like a Reynolds number, either gas or liquid, and a Weber number of the same phase along with liquid-to-gas ratios for velocity, density, viscosity and thickness. However, the examination of forces, given above, suggests a more meaningful selection. With this force-based approach only five nondimensional groupings are generated and the choice of the sixth grouping seems tricky since all of the forces appear properly accounted for. This final grouping could reflect additional aspects of atomization such as the finite lifetime of the film. For example, a ratio of the mass loss rate due to atomization to the mass flow rate of the liquid. Similarly, in injectors, where it is desirable to fully atomize the film within the injector, a ratio of atomization time to time within the device would be appropriate. In actuality, however, the exact mechanisms involved must be known before mass loss rates can be determined. With luck, a map can be developed in the future wherein the prior five groupings can be used to determine the dominant atomization mechanisms. In the absence of this guidance, however, a ratio of thicknesses, viscosities or Reynolds numbers is recommended. A final note in the choice of nondimensional groupings is the observation that the nine parameters given at the beginning of this paragraph account for most general atomization cases. In many of the mechanisms discussed in this paper additional parameters and, consequently, groupings, may become important if that mechanism is known to dominate. For example, if the prevailing mechanism is driven by gas-phase structures such as a recirculation zone behind a backward facing step [9] then the step height is an important parameter and the Reynolds number based on step height is an important grouping.

The choice of characteristic length and velocity scales used to calculate these groupings is still somewhat uncertain. The annular film literature mainly uses gas velocities and pipe diameters, partly because these values are often more accurately known than the film velocity and film height and partly because the film flow is generally laminar. Interface velocities are

sometimes used and, because atomization is a surface phenomenon, their use seems justified. Similarly, a strong argument can be made for using the relative velocity in some groupings, especially when aerodynamic effects are important. Practically, however, using either the interface or relative velocity is difficult because they are rarely known. The same difficulty exists if the disturbance height or even average film thickness is used as a characteristic length scale. In general, the exact choices of velocity and length scales will depend on the exact set-up and, to a lesser extent, the mechanisms involved. Luckily, recommendations can be made based on the literature and an understanding of what these groupings are trying to capture; the above suggestion of nondimensional numbers was formulated with the intent of making these recommendations. Accordingly, Reynolds numbers should use the velocity of the phase and its characteristic height; Weber number velocity should, ideally, be the relative or interface with the disturbance height as the length; Froude number should be based on disturbance height and velocity; kinetic energy ratio should be based on the velocities near the interface when available.

B. Quantitative Description of Atomization Mechanisms

Accurate descriptions of atomization mechanisms which are simple and well-defined enough for general use are limited. Usually, the entire process cannot be modeled except, perhaps, with a full numerical simulation; due to the time investment and specialized knowledge required to produce sufficiently detailed and accurate simulations, they are not practical in many situations. Some important, specific details of the atomization processes are attainable through the use of simplified theories. In particular, theories often focus on predicting the droplet sizes that would result from a particular atomization mechanism or the thresholds for determining when a mechanism is active. Most of the earlier-presented atomization mechanisms are revisited in this section. Available theoretical models and the process of their derivation are given. Many of these theories require additional correlations for particular values; these correlations are given as considered helpful. Additionally, some experimental work and simplified empirical correlations that result from experiments are reviewed. The reader is strongly encouraged to consult the citations for more details on these quantitative descriptions.

Liquid turbulence

Comparisons by Faeth and colleagues of atomization due to liquid turbulence in jets, annular sheets and annular films show striking similarities between the geometries [2, 18, 21, 23]. Consequently, expressions for droplet size, speed and the location of initial ligament and droplet formation which were derived for jets can also be used to describe film atomization. These expressions arise from an energy balance at the interface: a ligament is formed if the eddy has sufficient energy to overcome the surface energy of the liquid, i.e. $\rho_f d_e^3 v_e^2 \sim \sigma d_e^2$ [2, 18, 21, 23]. The ligament is assumed to share the characteristic size of the eddy that formed it; the smallest ligaments are of the Kolmogorov size scale or the scale of the smallest eddy with sufficient energy to form a ligament, whichever is larger. Their findings indicate that the eddy responsible for ligament formation is in the inertial range so that $v_e \sim v_{rms} (d_e/d_l)^{1/3}$ where the root-mean-square velocity is perpendicular to the bulk flow direction and d_l is the integral length scale, $d_H/8$. Combining these ideas yields an expression for ligament diameter $d_{lig}/d_l = c_1 (v_i/v_{rms})^{6/5} We_{fsl}^{-3/5}$ where $We_{fsl} = \rho_f v_i^2 d_l / \sigma$. Further, if the Rayleigh mechanism is assumed for ligament breakup then $SMD = c_2 d_{lig}$.

The turbulent boundary layer must develop and interact with the surface. The distance over which the boundary layer develops, assuming a $1/7^{\text{th}}$ velocity distribution power law based

on Schlichting's results, is $x_{BL}/d_H = 3.46(c_3\delta_f/d_H)^{5/4}Re_{fdH}^{1/4}$ where $Re_{fdH} = d_H v_{m,i}/\nu_f$. Once the turbulence reaches the surface the time required for the formation of a ligament is proportional to the diameter of the ligament divided by the velocity of the eddy. The distance, therefore, for ligament formation is $x_{lig}/d_l = c_4(v_i/v_{rms})^{6/5}We_{fdl}^{-3/5}$. Dai et al. [2] further develop this expression into $x_{lig}/d_l = c_5(v_i/v_{rms})^{9/5}We_{fdl}^{-2/5}$. The time for the breakup of the ligament via the Rayleigh mechanism is longer, however. Neglecting viscous effects, the Rayleigh breakup time is $\sim(\rho_f d_{lig}^3/\sigma)^{1/2}$, so the breakup length for Rayleigh instabilities is $x_R = c_5 v_i (\rho_f d_{lig}^3/\sigma)^{1/2}$. Overall, then, a film requires a distance $3.46d_H(c_3\delta_f/d_H)^{5/4}Re_{fdH}^{1/4} + c_4 d_l (v_i/v_{rms})^{6/5}We_{fdl}^{-3/5} + c_5 d_l (v_i/v_{rms})^{9/5}We_{fdl}^{-2/5}$ to begin to break into droplets that have a Sauter mean diameter $SMD = cd(v_i/v_{rms})^{6/5}We_{fdl}^{-3/5}$.

Note that in all of the above derivation aerodynamic effects were neglected. The authors of the derivation claim this is a good approximation if ρ_f/ρ_g is greater than 500 [2]. Sarpkaya and Merrill [48] calculate the aerodynamic force on the ligaments for their experiments in water and air. They give the drag force on a ligament as $F = (C_D \rho_g/2)(\delta_f v_i / \tau_m)^2 d_{lig} L_{lig}$. This force is approximately equal to 0.34g using $C_D = 1.2$ and values from their experiments. Note that τ_m is the local average film thickness. Using these values the torque on the ligament would be about 2.5mm*g which should be negligible.

Dai et al. [2] also reported the results of experiments on annular films of turbulent liquids. Their experimental conditions were outer wall films with inner diameters of 6.4 or 50.8 mm which were in the neighborhood of 1.5 to 5 mm in thickness. Their working fluids were water, glycerols and ethyl alcohols such that their Reynolds numbers varied from 17,000 to 840,000 and their Weber numbers varied from 6,100 to 57,000 (based on film properties and hydraulic diameters). Their density ratio was always about 500, so aerodynamic effects were neglected. The hydraulic diameter was calculated as $d_H/\delta_f = 4(1 + \delta_f/d_{rod})$. Based on the above derivations data was plotted against We_{fdl} and correlations were developed for SMD and the distance for the onset of breakup. $SMD/d_l = 109 We_{fdl}^{-0.61}$ while $x_{BL}/d_H = 0.061 Re_{fdH}^{1/4}$ and $x_R/d_l = 7100 We_{fdl}^{-0.54}$. The time for ligament formation is neglected as small.

Rein [92] takes a slightly different approach to droplet formation and equates the eddy energy with the droplet energy, so that the eddy energy is equivalent to the surface plus kinetic energy of the droplet. He assumes that the droplet size is equal to the eddy size. His formulation is motivated by a desire to understand the creation of droplets with sufficient energy to entrain air in channel flows. This approach yields an equation for droplet size: $(\pi/6)d_d^3\rho v_{rms}^2/2 = \pi d_d^2 \sigma + (\pi/6)d_d^3 \rho v_{in,d}^2/2$. He goes on to estimate v_{rms} by arguing that it is approximately equal to the friction velocity in the gas and using the law of the wall to relate the friction velocity to the inlet velocity. Further, he assumes the film is thin and that the film thickness is the distance from the wall. Instead of droplet sizes, the energy balance can be used to generate an equation for droplet Weber number, $v_{rms}/v_{in,d} = (1 + 12/We_{in,d})^{1/2}$, where $We_{in,d} = \rho v_{d,in}^2 d_d / \sigma$. This equation is useful for considering whether the created droplets meet critical Weber number demands for particular behavior, such as air entrainment. Theoretically, the largest droplets will occur when their initial velocity is zero, but droplets will only separate if the apex of their trajectory is greater than $v_{in,d}/(2g)$.

Experiments [48] show that about 10% of droplets created by liquid turbulence in quiescent air appear to be created by a separation at the film surface. This separation may be caused by the interaction of turbulent eddies with the base of the ligament [48]. A droplet resulting from this type of breakdown would have a volume equal to that of the ligament. An expression for droplet diameter can be generated by equating these two volumes,

$d_d = (3d_{lig}^2 L_{lig}/2)^{1/3}$. Using the peak values (for the middle roughness) from the experimental results of by Sarpkaya and Merrill [48] d_{lig}/δ_f is about 0.32, L_{lig}/δ_f is about 4.8 and d_d/δ_f formed by the Rayleigh mechanism is about 0.56. If the entire ligament was severed d_d/δ_f would be 0.90, about a 50% increase over the droplet diameter formed via the Rayleigh mechanism. Note that these values are for a flat water film 5.4 to 15 mm in depth flowing with an initial liquid velocity of 6.2 m/s; the surrounding gas is quiescent air.

Hydrodynamic instabilities

Hydrodynamic stability can, theoretically, be used to predict the wavelength and growth rate, hence the size, of wave disturbances on the surface of the film. In practice, there are numerous difficulties to accurately predicting these values. Many of the difficulties have been outlined above, but in summary the equations to describe hydrodynamic stability are complex and nonlinear, lacking analytic solutions. To simplify the equations and allow analytic or rapid numeric solutions assumptions must be made; unfortunately, there is doubt about how simplified the problem can be made and still yield accurate results. Comparisons of various simplified theories and experimental data are favorable [69, 73], however. Better agreement comes from fewer assumptions and, therefore, more complex formulations. To this end several tools and codes have been developed to deal with hydrodynamic instability formulations. A commonly available tool for sheets is LISA. LISA has been successfully implemented in conjunction with other numerical descriptions of the entire atomization process to help predict spray characteristics of pressure-swirl atomizers—a specific type of atomizer which produces a thin, almost conical sheet [32, 98]. Because LISA refers to a sheet, however, it assumes two deformable boundaries and atomization through a Sheet Pinching phenomenon. A similar, commonly used and available tool for film atomization does not currently exist.

Once a formulation for hydrodynamic stability is derived it is solved to find curves of neutral stability and, for unstable systems, the most rapidly growing wave (as time or distance becomes infinite). This wave is considered to be the important and dominant wavelength of the system [58]. To further complicate the determination of wavelengths and sizes from unstable films, recent work suggests that the most unstable wave at infinitely long times/distances is not always the dominant wave [52-54, 67]. Yecko and colleagues suggest that waves which are stable at infinite times may have very large growth rates at short times and, because atomization often occurs over short times/distances, these initially fast growing waves dominate the atomization behavior. This theory suggests that waves could appear on films which are stable according to the hydrodynamic stability formulations; due to the wider range of conditions over which this theory would predict waves it seems recommended for decisions on whether the interface will be smooth or wavy. Occasionally, these hydrodynamic stability or temporal growth formulations can be solved analytically, but most require some amount of numerical solution.

In view of the other uncertainties in the atomization process it is not clear how important the choice of models that predict wave characteristics is nor which model is best suited for a particular set of conditions. The required accuracy of the wave description is difficult to assess. Due to these problems and the large number of unique formulations available in the literature no presentation of formulations or results are given here. Instead, the reader is referred to the book by Drazin and Reid [70] or the references contained in the earlier section on hydrodynamic instabilities for specific formulations and results.

Ostrach and Koestel [69] have presented a simple method for predicting the onset of breakup in a hydrodynamically unstable film. The model relies on a number of assumptions. Two are commonly found throughout stability works—the wave with the maximum growth rate dominates and linear stability theory is sufficient to describe the flow up until atomization. They also assume that the earliest formed wave is the one that is important and confine their attention to the evolution of this single wave. The wave and interface speeds are assumed to be constant with no relative motion between the liquid and the interface. The length a wave has traveled at any time is then given by $L=t(v_i+v_w)$ so that $dL=v_w(1+v_i/v_w)dt$. A further assumption, that the velocity at the interface is much greater than the wave speed, allows the development of a vertical velocity equation, $v_{vert}=dh/dt+v_i dh/dL$ where h is the total height of the disturbance. A simple linear stability analysis gives a different expression for the vertical velocity $v_{vert}=-ikf(h)\exp\{ik[1-(v_w+iv_{img})t]\}$ where $f(h)$ is an unknown function of height such that the stream function of the flow is equal to $f(h)\exp\{ik[1-(v_w+iv_{img})t]\}$. The two expressions for vertical velocity can be equated. If the disturbance velocity, f' , is much less than the total wave velocity (v_w+iv_{img}) then this equation can be simplified to $d^2h/dt^2=kv_{img}(dh/dt)$. Defining the wave height h_w as the difference between the total height and the film height, $h_w=h-\delta_f$, yields (after some manipulation) $dh_w/h_w=kv_{img}dt$. Combining earlier expressions this results in an equation for the wave height $dh_w/h_w=kv_{img}dL/[v_i(v_w/v_i+1)]$. This expression can also be written as $dh_w/h_w=\omega dL/[\delta(v_w/v_i+1)]$ where ω is a growth rate parameter equal to $kv_{img}\delta/v_i$. Either of the expressions for dh_w/h_w should be integrated from $L=0$ to L_b and $h_w=h_{w,in}$ to $h_{w,b}$ to get the location (length) of breakup as a function of the wave height at breakup. Application of these results is hampered by, among other things, the difficulty in accurately determining the growth rate parameter or wave number from stability theory as well as an incomplete knowledge of the wave height at breakup. Wave stripping mechanisms suggest several possibilities for wave height at breakup which could be used with this theory and any of the myriad hydrodynamic stability models to predict the length needed for the onset of breakup.

Gas vortices

The effect of gas vortices on an interface has not been examined quantitatively in the literature. Parallels with liquid turbulence can be drawn, however. An energy balance at the surface interface can be performed with the assumption that the interface will deform if the vortex has sufficient energy to overcome the surface energy of the liquid, $\rho_g d_e^3 u_e \sim \sigma d_e^2$. Notice that this expression and logic is similar to that used in liquid turbulence work [2, 18, 21, 23, 92] except that the fluid density and velocity have been replaced by their gas values. The implication of the energy balance is that some critical We based on the characteristic vortex diameter and viscosity exists at which deformation of the interface occurs. Unlike the liquid turbulence case the eddy would not produce a ligament with a diameter equal to its characteristic size. Instead the eddy would deform the surface either by creating an indentation or pulling liquid up in the direction of its rotation or, most probably, some combination of the two. If the gas layer was thin, of comparable size to these vortices, indentations and structures similar to the liquid turbulence case (but with the phases reversed) might appear. More likely, however, the vortices would not be of a size of the gas layer thickness and their deformation of the interface would depend on their bulk motion relative to the film, e.g., an eddy moving rapidly towards the interface would be more likely to cause a depression while an eddy whose motion was largely along the interface might cause more lifting and stretching of the surface. Also, there are situations in rocket engines in which the surface energy may not be the limiting factor, e.g. as

pressure or temperature increase to near the critical point. When surface energy is negligible the eddy or vortex energy would need to overcome the gravitational and/or inertial energy of the liquid in order to cause deformation. Most of this process remains conjecture at this time awaiting further numerical and experimental studies of the effects of gas vortices on liquid interfaces.

Pressure fluctuation

If pressure fluctuations cause a change in mass flow rate then a wave can be “artificially” created. A simple approximation of the change in film height can be made by neglecting any acceleration of the flow and assuming that the change in mass flow rate is initially felt only over a short distance L_w . Define a control volume from the start of the film to L_w and over the entire film width W . The inlet mass flow rate will be $m_f + \Delta m_f$ while the exit flow rate will still be m_f . Using conservation of mass, then, $\Delta m_f / \rho_f = WL_w h_w / \Delta t$ where h_w is the change in film height over the time interval Δt that the mass flow is at the increased level. The length of the control volume is essentially the length a particle of fluid traveling at the (new) film velocity can travel over the time interval of increased flow, $L_w = v_f \Delta t$ with $v_f = (m_f + \Delta m_f) / (\rho_f W h_{gap})$ where h_{gap} is the height of the film inlet (where the free surface starts). Combining these equations yields an expression for the disturbance height as a function of the change in mass flow rate $h_w / h_{gap} = 1 / (m_f / \Delta m_f + 1)$. If the wave were to remain the same height and length as when it was formed, it would travel with the original film velocity, i.e. that associated with m_f . This last condition seems unlikely, however, as the surface tension and aerodynamic forces are likely to alter the wave’s shape as it progresses downstream.

Woodmansee and Hanratty [93] present a simple theory for determining if a disturbance such as this will separate from a film. While this theory essentially describes a stripping process it is included here due to its focus on pressures and ability to account, in some regard, for the effects of fluctuations in feed and environmental pressures. The theory is based on a comparison of the suction created by the gas flowing over a curved surface with the surface tension force at the interface. If the surface tension force is larger than the suction then the disturbance will remain a part of the film; if the suction force is larger then part of the disturbance will separate from the film. They give expressions for the pressures generated by each of these forces. For suction over a wave $p_g = \rho_g (u_g - v_w)^2 (h_w / L_w) f(h_w / L_w, h_w / h_g)$ where f is an unknown function. The pressure change due to surface tension is $p_\sigma = f_2 \sigma h_w / L_w^2$ where f_2 is another unknown function. There will be separation if $p_g > p_\sigma$, or, in other words, if $f L_w \rho_g (v_g - v_w)^2 / \sigma$ is above a critical value. This specific critical value as well as a form or value off is not reported. Additionally, L_w and v_w may be difficult to calculate and may need to be experimentally measured as in Woodmansee and Hanratty’s analysis [93].

Splashing

The literature gives a variety of conditions to determine when an impacting droplet will splash. The most common condition is the Sommerfeld condition which determines if a crown will form from droplet impact. The Sommerfeld condition is a lower bound on the parameter $K = We_d^{1/2} Re_d^{1/4}$ with both nondimensional numbers based on the droplet velocity and droplet diameter, i.e. $Re_d = \rho_d d v_d / \mu_f$ and $We_d = \rho_d d v_d^2 / \sigma$ [108]. The bounds on K are from tens to hundreds with a general value around 50 [108]. Samenfink et al. [109] set the limiting condition as a minimum droplet momentum at impact. They do not give values for this momentum but give the limiting droplet velocity for splashing as 12.5 m/s for 100 μm droplets of water impacting at 45°.

These conditions yield a limiting momentum around 4.5 nNs. Pan and Law [107] give the controlling parameter for whether the droplet bounces, splashes or coalesces as the Weber number of the droplet based on impact velocity. They also determine that film thickness only plays a role if it is less than the droplet radius.

Predicting the sizes of droplets created by splashing is difficult because the mechanism by which the ejected sheet breaks into ligaments is not clearly understood [122]. A further complication is the jet that may form when a droplet impacts a film; whether this jet forms and, if it forms, its height and width are functions of the film thickness as well as the size and velocity of the impacting droplet [123]. A simple theory to predict the size of crown droplets formed from the impact of a droplet with a dry wall is given by Wu [122]. He assumes each jet is formed from an element of the ejected sheet of thickness δ and circumferential length L . A mass, energy and momentum conservation is then established between this sheet element and the resulting ligament. The three conservation equations can be solved approximately for d_j/δ and v_j/v_s , but the velocity of the sheet, v_s , remains unknown. To get this velocity Wu uses an energy conservation during droplet impact equating the kinetic and surface energy of the impacting droplet with the sum of the kinetic energy, surface energy and viscous dissipation in the sheet. The viscous dissipation is approximated in the crown only. If the formed ligaments are assumed to break up via a Rayleigh mechanism, the ligament size is directly proportional to the created droplet size ($d_{d,cr}=1.889d_j$). All of these results are combined to yield an equation for the secondary droplet size in terms of the Weber and Reynolds numbers of the impacting droplet: $d_{d,cr}/d_{d,in}=[4.23/(We_d+12)][(9+2We_d(We_d+12)/Re_d)^{1/2}+3]$. Wu [122] notes that this model should also apply to the case of a wet wall, but does not consider the possibility that part of the film liquid could be pulled into the crown sheet.

Splashing has generally been investigated as droplets impact walls or still films, but the case of interest in many atomizers is droplets impacting moving films with an imposed gas velocity. Samenfink et al. [109] examine the impact of droplets on shear driven liquids which, in general, are wavy. They find that the droplet generally impacts the back of the waves due to the imposed gas flow, but that the results of the impacts are the same as with flat films, provided the correct impact angle is used, for impact angles $< 20^\circ$. They also give empirical correlations for the size and velocity of produced droplets. They find that the distribution of sizes and velocities is log normal. For the created droplets, the normalized size is given as $d_{d,m}/d_{d,in}=1.0-0.03454s_c^{0.175}\alpha^{0.1239}La^{0.265}$ and the normalized velocity is given as $v_m/v_{in,d}=0.08214s_c^{-0.3384}\alpha^{0.2938}La^{0.1157}(\delta/d_{d,in})^{-0.03113}$. The normalized momentum of the resulting droplet is given as $s_c=(1/24)Re_dLa^{-0.4189}=(\rho d_{d,in})^{0.581}v_{in,d}(\sin\alpha)^{0.63}/(24\mu^{0.162}\sigma^{0.4189})$; it is normalized by the critical momentum to cause splashing. The Laplace number is $\rho_f\sigma d_{d,in}/\mu_f^2$. The correlation is good for $1 < s_c < 5$, $0.3 < (\delta/d_{d,in}) < 3$, $5000 < La < 20000$ and $5^\circ < \alpha < 90^\circ$.

Bubble Bursting

Bubble collapse is a complicated mechanism and no simple theory exists to approximate the droplets produced by the rupture. As discussed above, when bubbles break they produce numerous film droplets and a few jet droplets. Due to the small sizes of film droplets (order of μm), they are rarely measured and generally not considered important for single bubble bursting. Jet droplets, however, have been studied both numerically and experimentally [103-105]. In order to discuss the results of bubble collapse, something about the size and number of bubbles in the flow must be known, however. Rodriguez and Shedd [91] experimentally study the bubble entrainment in horizontal, annular flows of compressed air and filtered water. Gas flow

rates were 200 to 700 l/min and film flow rates were 0.2 to 1.5 l/min. They observed that bubble entrainment was due to wave action, particularly waves breaking. Their bubble counts for a 15.1 mm inner diameter tube were on the order of 100 per cm² and mean bubble diameters were 12 to 26 μm , depending largely on air flow rate.

Duchemin et al. [105] examines the relevant forces and scaling in bubble collapse. Bubble bursting depends on the viscosity, density and surface tension of the liquid as well as gravity. These parameters can be combined into two different length scales, a capillary length scale ($R_c=(\sigma/\rho_f g)^{1/2}$) and a viscous-capillary scale ($R_v=\rho_f v_f^2/\sigma$). If the bubble radius, R_B , is much less than R_c then capillary effects are much more important than gravity effects. If the R_B is much larger than R_v then viscous effects are much less important than capillary effects. If both of these criteria are met ($R_v \ll R_B \ll R_c$) then surface tension and inertia dominate the bursting event. For water the capillary length is 2.7 mm while the viscous-capillary length is 0.014 μm [105], so many droplet-producing bubbles would fall within this surface tension and inertia dominated range.

Several predictions and measurements of resultant droplet sizes exist. Experimental results indicate that jet droplet diameters are generally on the order of 10% of the bubble diameter [104, 105]. The numerical results of Duchemin et al. [105], in the range where viscosity effects are negligible, predict the jet droplet radius is about 13% of the bubble radius; bubbles with radii smaller than the range where viscosity is negligible produce droplets that are even smaller, in the range of 2% of the bubble radius for $R_B/R_v \sim 1 \times 10^3$. Günther et al. [104] present a compilation of experimental findings in a plot of ejected droplet diameter versus bubble diameter (as well as a matrix of experimental findings). The graph can be roughly fit by a line indicating the jet droplet is about 10-20% of the bubble size; more accurately, however, there appear to be two different behaviors, one for bubbles under about 1 mm and one for larger bubbles. The experimental results of Günther et al. [104] show that a bubble of 2.98 mm generates an average droplet 0.525 mm in diameter, about 17% of the bubble diameter. They also give a size correlation for the case of multiple collapsing bubbles: $d_d=3.341/d_B^{3/2}$.

Other parameters for droplet production from bubble collapse are important but less well studied. Georgescu et al. [103] calculate jet ejection speed, which varies dramatically with bubble size. For bubbles 35 μm in radius they calculate ejection speeds of 80 m/s while for 1 mm bubbles this speed is only 3.5 m/s. They also look at ejection times for the jet produced by a bursting bubble and find it to be on the order of milliseconds. This finding is particularly important because in order to produce a droplet the bubbles have to rise to the surface, burst and produce a jet which must then break down. The studied rocket injector nozzle cited previously [10] was less than 10.0 mm in length and the liquid traveled toward the exit at speeds on the order of 1 m/s [10], so a bubble traveling with the liquid would remain in the nozzle for less than ten milliseconds. This appears to be just enough time to produce a droplet provided the bubbles were already present in the flow. In further support of the possibility of bubble collapse within the rocket injector, the collapse times reported by Georgescu et al. [103] are for bubbles with initial diameters of 0.5 mm. The experimental work of Rodriguez and Shedd [91] suggests bubbles in horizontal annular flow with large gas velocities will be an order of magnitude smaller, on the order of tens of μm . Smaller bubbles have shorter ejection times, so bubble bursting certainly cannot be ruled out as occurring in rocket injectors, although it may be a secondary effect in terms of atomizing the entire film. Finally, Günther et al. [104] present correlations for the number of droplets produced. An early correlation for the number of film

droplets is given as $N_{Fd}=5/3(1000d_B)^{5/3}$ for bubbles from 0.8 to 500 μm . A correlation for the number of jet drops is $N_{Jd}=7.5\exp(-1000d_B/3)$.

Hole growth

Theoretical developments exist in the literature to determine whether a stable unwetted area will form in a flowing film subjected to a gas flow [94, 112]. These stability criteria are generally given as a minimum liquid flow rate or film thickness. The criteria state that if a hole is formed and the liquid flow rate or film thickness is below the critical value then the hole will not close and/or be swept downstream. Another set of criteria determine whether this dry patch grows or remains a stable size. The rate of growth of the hole in a moving fluid has received little attention despite the vast array of literature on hole growth in stagnant films [111, 113]. Further, as with wave coalescence, there are no details on how colliding rims produce air borne droplets. Droplets may be produced in ways other than collision of rims, however. For example, flow over the curved rim will lower the pressure over that section of the film and may lead to a piece of the rim separating from the wall. The criteria for this could follow Woodmansee and Hanratty's [93] formulation detailed in the pressure fluctuation discussion above. As a result of these various factors, the only portion of hole formation discussed in detail is the stability criteria for hole production.

Two main approaches exist for determining the stability of a dry patch in a shear driven film. Penn et al. [94] use a force balance at the contact point of the film, wall and gas while Saber and El-Genk [45] use a minimum total energy approach, assuming division of a rivulet occurs when its total energy is a minimum. Penn et al. [94] consider four force components: inertia of the liquid, gravity, surface tension and shear. They must make further assumptions to determine the forces: the flow in the film is a Couette flow, $v_f=v_f(y/\delta_f)$, the shear at the liquid-solid interface goes to zero at the stagnation point of the hole, the liquid-gas shear force remains constant over the control volume and the flow is fully developed at some point upstream of the hole so that the liquid-gas and liquid-solid shear stresses are equal and opposite there. Their final force balance is $\rho_f\delta_f v_f^2/6+L\tau_{gf}/2=\rho_g\delta_f L+\sigma(1-\cos\theta)$ which is inertia + shear = gravity + surface tension forces where L is the length over which the shear stresses are not in equilibrium and is also the length of the control volume. If the left-hand side of the equation dominates then the dry patch is washed away; if both sides are equal the dry patch remains constant; otherwise, the dry patch grows. If surface tension and shear dominate then a single nondimensional parameter gives the stability criteria, $\sigma(1-\cos\theta)/(L\tau_{gf}/2)$. Application of this criterion is hampered by the inclusion of the gas-liquid shear and length over which the shear changes. Penn et al. [94] use the empirical formula of Henstock and Hanratty [124] for laminar flow to determine the liquid-gas shear, $\delta_f(\tau_{gf}/\rho_f)^{1/2}/v_f=1.414Re_f^{1/2}$. The film Reynolds number, Re_f , is equal to $\rho_f v_f \delta_f / \mu_f$. They use a numeric simulation to determine a value for L and cautiously give an empirical correlation $L\approx 0.84W_{dp}$ where W_{dp} is the width of the dry patch. Substituting this relation into the stability criteria gives a relation between the flow rate and thickness of the film for stability. In the surface tension-shear dominated regime this corresponds to stability or closure when $\sigma(1-\cos\theta)\delta_f/(dv_f/\mu_f)\leq c$ where c is of the order of 1.

Saber and Genk [112] use the minimum total energy approach and consider only the kinetic and surface energy of a rivulet. (Their results show that these rivulet calculations may be used to predict breakup of wider films.) This formulation requires the velocity profile of the rivulet and the shear stress at the interface to be known. They use the Navier-Stokes equations and the Ritz method to determine the flow within the rivulet. A combination of the Laplace-

Young relation and the momentum balance normal to the rivulet surface allows the rivulet profile to be calculated. They use a correlation for the shear stress, $\tau=0.5f_i\rho(u_g-v_i)^2$ [125] with $f_i=0.006+2\times10^6\delta/\phi(\mu/\mu_r)^{-0.44}$ where ϕ is the rivulet profile and μ_r is a reference viscosity equal to 1 cP [126]. These relations are substituted into the energy equation, its minimum is found and the result is solved for the film thickness giving the minimum stable film thickness. To calculate the minimum flow rate the velocity and rivulet profile can be substituted into a volumetric flow rate equation using the afore-calculated minimum film thickness. The results of these calculations are quite complex, however, and are not reproduced here. Comparisons for the case with no gas flow indicate that the minimum energy results are more accurate than force balance results [45].

Stripping

Numerous theoretical descriptions of aerodynamic stripping mechanisms exist. The prediction of when and how much liquid will be stripped necessitates some assumptions. Assumptions utilized in the literature include 1)assuming the size of the created droplets is similar to the wavelength of the stripped wave [101], 2)equating the aerodynamic pressure drop with the pressure due to surface tension [93], 3)balancing gravity, drag and surface tension forces [43] and 4)conserving energy in the film and droplet before and after stripping [118]. The pressure equality assumption (2) of Woodmansee and Hanratty [93] has already been presented in the section on pressure fluctuations; theoretical descriptions based on the other three assumptions are presented below.

Maroteaux et al. [118] equated the energy of the film prior to droplet production to the energy of the film plus the energy of the droplet following production. They assumed that the energy was composed of a surface energy and a kinetic energy only. In order to determine the minimum energy necessary for droplet formation they set the kinetic energy of the droplet to zero. The wave height in time and space is set equal to $h_w(t)\sin(2\pi x/\lambda)$. If the wave velocity remains constant in the propagation direction then $v_w=\omega h_w$. Assume also that the mass stripped from the wave corresponds to half the wavelength. (Similar to the assumption of Mayer [101] discussed below.) The energy balance is determined using these equations and assumptions: $\rho_f\lambda\omega^2h_w^3/(3\pi)+(\sigma/2)f=\sigma\lambda/2+\sigma\pi d_d^2/L_w$ where $f=\int_0^{\lambda/2}1+[(2\pi h_w/\lambda)\cos(2\pi x/\lambda)]^2dx$ and L_w is the wave width. They examined two different widths: $L_w=h_w$ and $L_w=\lambda$. For the conditions tested by Maroteaux et al. [118], corresponding to films in the cylinders of port fuel injected engines, this theory predicts no or little aerodynamic stripping. Application of the theory is somewhat difficult, however, because the maximum growth rate, wave length and wave height must be known. Maroteaux et al. [118] predict these values using a linear hydrodynamic stability analysis wherein they find the disturbance amplitude and velocity are not negligible compared to the mean flow which raises serious doubts about the use of a linearized analysis.

Mayer [101] used the assumption that the droplet stripped from a wave has a diameter proportional to the wavelength of the wave. He was particularly focused on capillary waves, but his derivations can easily be extended to gravity waves. He uses results reported in Lamb's [127] text for the speed of capillary (and gravity) waves: $v_w=(\sigma k/\rho_f)^{1/2}$ (or $v_w=(g/k)^{1/2}$). An energy balance for a wind driven wave is reported in Lamb, $dh/dt=[\beta\rho_g v_{rel}^2 k/(2\rho_f v_{wave})-2\mu k^2/\rho_f]h$. If the gas and wave velocities are assumed to be constant, the bracketed term is a function of wave number only or, more conventionally, wavelength only. Mayer calls the bracketed term, in terms of wavelength, a reciprocal time modulus, $1/\tau$. (At this point in the derivation Mayer [101] assumes the gas velocity is much greater than the wave velocity and replaces v_{rel} with v_g ; this

simplification is not necessary for solution, however.) The minimum maintained wavelength, λ_{min} , will occur when $1/\tau=0$. The rate of atomization mass flux over the wavelength range of λ to $\lambda+d\lambda$ is given by $m''d\lambda \sim \rho_f \lambda d\lambda (1/\tau)$ and the droplet formation rate is $\rho_f \lambda^3 n'' d\lambda \sim m'' d\lambda$ due to the assumption that waves break down as their amplitude reaches a value equal to their wavelength. Consequently, neglecting the proportionality coefficient that accounts for the wave shape, $n'' d\lambda \approx d\lambda / (\lambda^2 \tau)$ at steady state. This relation can be used to determine the mean wave length $\lambda_m = 9\lambda_{min}/2$ (utilizing $\sum n''/\sum n'' = \lambda_m$ with the sum taken over all wavelengths). Going back to the initial assumption about droplet size, $d_{d,m} \sim \lambda_m$, and using the relations given above the mean droplet diameter is $d_{d,m} = 18\pi(c/\beta^{2/3})[\mu_f(2\sigma/\rho_f)^{1/2}/(\rho_g v_{rel}^2)]^{2/3}$. The parameter $c/\beta^{2/3}$ must be determined experimentally. For jets Mayer [101] finds that c weakly depends on $\mu_f^{-1/3}$, but if assumed to be constant $c/\beta^{2/3} \approx 0.3$. The analogous result for gravity waves, not given by Mayer, is $d_{d,m} = 9\pi(c/\beta^{2/3})[2\mu_f(g)^{1/2}/(\rho_g v_{rel}^2)]^{2/3}$. Strakey et al. [10] makes use of Mayer's [101] capillary stripping mechanism to predict the mass flux per interfacial area and film dry-out times. They get a mass entrainment flux $m_e'' = c_1 [\mu_f \rho_f (\rho_g v_{rel}^2)^2 / \sigma]^{1/3}$. (The equivalent for gravity waves would be $m_e'' = c_1 [\mu_f (\rho_g v_{rel}^2)^2 / g]^{1/3}$.) They also give the dry-out time as $t_{dry} = m_f / (m_e'' P v_f)$ with $m_f \approx \rho_f v_f d_{pipe} \delta_f$.

Holowach et al. [43] take a different approach by assuming that the maximum droplet size occurs when the sum of forces acting on a piece of the wave is equal to zero. They assume that the wave has a three-dimensional sine-wave profile and consider the drag, gravity and surface tension forces on a wave traveling upward in a vertical pipe. The drag force is $F_{drag,x} = \rho_{g,BL} C_D A_{en,w} v_{rel}^2$ where $\rho_{g,BL}$ is an average of the gas core and vapor densities and $A_{en,w}$ is the cross-sectional area of the part of the wave which is stripping. Using a two-dimensional sinusoidal cross section for illustration, i.e. $y = h_w \sin(2\pi x/\lambda)$, they calculate $A_{en,w} = (h_w \lambda / \pi) \cos(2\pi b/\lambda) - h_w (\lambda/2 - 2b) \sin(2\pi b/\lambda)$. The parameter b represents the distance in the y -direction from the wave trough ($x=0$) to the point where the stripped area starts; b is the parameter for which the force balance equation is solved. Both h_w and C_D are unknown; Holowach et al. [43] determine these values based on correlations available in the literature. The gravity force on the wave traveling vertically upward is $F_{grav,x} = -\rho_f V_{en,w} g$ where $V_{en,w}$ is the volume of the entrained wave. Several additional assumptions are needed in order to calculate the surface tension force. This force is assumed to be due to wave deformation only (i.e., the wave is symmetric and the force is zero with no deformation); the average curvature of the wave crest is assumed to be equal to the curvature at the peak of the sine wave; the wave is assumed to flatten at the rear so that the surface tension force acts on the front only; and, finally, the tension is assumed to act over a circle with the diameter $\lambda/4-b$. (Helpful diagrams and additional information can be found in Holowach et al.'s paper [43].) This leads to a surface tension force of $F_\sigma = \sigma \pi^3 h_w (\lambda/4-b)/\lambda^2$ which acts at an angle determined by the slope of the sine wave. Consequently, the force is the direction of interest, x , is $F_{\sigma,x} = (\sigma \pi^3 h_w (\lambda/4-b)/\lambda^2) \cos \{\arctan[(2\pi h_w/\lambda) \cos(2\pi b/\lambda)]\}$. When the equations for these three forces are combined, a complex equation for b results. Once b is determined $V_{en,w}$ can be calculated. Holowach et al. [43] then use $V_{en,w}$ to determine the entrainment mass flux of the liquid per area of the control volume $m_{en}'' = V_{en,w} \rho_f N_{w,cv} / (A_{cv} t_{en,cv})$. The area of the control volume is approximately $A_{cv} \approx P \lambda (1-VF_f)^{1/2}$. The entrainment period for the gas, $t_{en,cv}$, is estimated as the time for the gas to flow over the film $t_{en,cv} = \lambda/v_{rel}$. Finally, the number of waves per control volume is $\sim P/\lambda$ which results in $m_{en}'' = V_{en,w} \rho_f v_{rel} / [\lambda^3 (1-VF_f)^{1/2}]$. While not presented by Holowach et al. [43] the relation of $V_{en,w}$ to b based on the three-dimensional sine-wave

geometry is $V_{en,w} = h_w[(\lambda/\pi)\cos(2\pi b/\lambda)]^2$. Setting this entrained volume equal to that of a sphere gives a resulting droplet diameter. Application of these results is hampered by the requirement of the wavelength and the entrained volume fraction, both of which are generally unknown.

Bag Breakup

While no quantitative theory for bag breakup in films exists in the literature, descriptions of other mechanisms may be utilized to develop an incomplete account of the process. The theory of Woodmansee and Hanratty [93] for the lifting of a ligament may be used to predict the onset of one type of bag breakup; this theory is outlined above. The other event leading to the beginning of bag breakup, undercutting of the wave, is not yet sufficiently understood or studied for predictions of its onset to be made. Bag growth can be predicted using a balance of aerodynamic forces due to flow over and into the bag with surface tension forces. However, this would require some knowledge or assumptions about the bag shape, speed and the size of the opening. With few experimental pictures, determination of good assumptions remains challenging. Assuming a hemispherical bag with an opening of a particular angle of the hemisphere along its upper edge is one possible, simple starting point. The rupture of the bag portion likely results in droplets of similar size and number (per equivalent surface area) to bubble rupture; yet, bag droplets may be somewhat larger due to thicker films at rupture. The bag will be thicker than a bubble due to the greater forces on the bag. Therefore, the main contribution to droplet size distribution will be the breakup of the large ligament which forms the leading edge of the bag. This ligament will likely breakup via the Rayleigh mechanism; if the diameter and length of the ligament prior to rupture can be determined then the resultant droplet size can be concluded.

Shattering

The only references to fragile shattering found in the literature suggests the phenomenon in secondary droplet breakup in centrifugal or other nonuniform velocity fields [100, 102]. Khavkin [100] approximates the breakup by assuming that these droplets deform into microcylinders prior to their shattering. Consequently, it seems reasonable that ligaments, which resemble cylinders, may undergo shattering if subjected to sufficiently large unsteady forces. For shattering to occur the stress in the cross section of the cylinder must be above a certain value. Khavkin's [100] gives this stress in terms of the centripetal force at a particular location, the exit area: $\tau = F_{cen}/A_{cs,lig}$. For a potential vortex flow, for example, $F = \rho_f A_{cs,lig} L_{lig} v_{in}^2 / R$ where R is a characteristic length for determining the velocity, say the exit radius or the radius to the interface. In a more general nonuniform flow the force can probably be approximated using the average velocity along the ligament. There is an obvious problem at this point—the length of the ligament depends on how the ligament was formed and is, in the vast majority of cases, unknown. The time scale of changes in the velocity field often remains unknown as well. Additionally, the stress at which shattering will occur is unknown. For droplets subject to centripetal forces Khavkin [100] found that fracture occurred if the stress was greater than or equal to 0.1 Pa. Whether this relation holds for all ligaments is unknown and quite unlikely. Clearly, further studies are needed to ascertain if and under what conditions ligament shattering occurs.

Film Separation

Maroteaux et al. [118] consider film separation as a result of Rayleigh-Taylor instabilities around a corner. This mechanism results in a sheet-pinching type of breakup. They develop a simple temporal linear stability analysis to predict wavelengths at a corner. Assuming rotating block motion for the film ($t_{pass} = \theta_{edge}\delta/v_f$) they formulate the critical corner angle at which separation will occur as $\theta_c = (v_f/\omega\delta)\ln(h/h_{in})_c$ where h is the disturbance height and h_{in} is the initial disturbance size. Unfortunately, both the maximum growth rate and the critical normalized disturbance height are difficult to obtain. They find good agreement with their experiments if a value of 20 is used for $(h/h_{in})_c$. The separated film forms one ligament per wavelength (of the wave with the maximum growth rate) and this ligament breaks down via a Rayleigh mechanism. The droplet diameter is, therefore, $d_d = 3.78(\lambda\delta/\pi)^{1/2}$. Again, application of this result is limited by the difficulty in determining the appropriate wavelength. Later work by Wang et al. [128] suggests, however, that for liquid film flow rates of 1 cm²/s and gas flows up to 60 m/s this type of separation does not occur. Wang et al. recommend a force balance on the film at the corner. Simplified force balances have been used to predict at which corners and flow rates the film will separate and become a sheet. This balance basically results in a Weber number criteria for separation [128]. Unfortunately, prior force balances are limited and do not take into account the effects of wall angle or, in many cases, gravity. Experiments show a definite dependence on corner angle and that gravity effects are important in flows with Froude numbers greater than unity [128].

C. Empirical Correlations

Because of the difficulties and limitations in application of simplified theories, extensive experimental testing is often required to ascertain the atomization behavior of devices. These tests are often undertaken with the hope of generating a correlation to predict important metrics. These metrics vary depending on the application. For cooling tubes, where the vast majority of literature and correlations exist, an important metric is the rate of entrainment and, more difficult to measure and correlate, the film thickness. For rocket injectors these two metrics may be of less importance; here droplet sizes are often considered important. An exhaustive review of empirical correlations is nearly impossible as different correlations exist for each geometry and range of flow conditions. This lack of universality led Roberts et al. [97] to observe that “This is perhaps because their correlations do not reflect the fundamental mechanism”. The scope of this review will be limited to a few more recent or widely used correlations for droplet size and entrainment rate focusing on the logic of their development. This section closes with a review of the experimental datasets available in the literature cited within this paper.

Most of the available correlations are for annular film flow of the type found in cooling tubes, predominately vertically upward flow. Application to rocket injectors is hampered because they are likely to operate at conditions not included in the experimental datasets for which the correlations are derived, e.g. higher gas and liquid velocities and smaller tube diameters. Early work was often focused on predicting quantities when equilibrium was reached, i.e. when the mass deposition and entrainment were equal. Equilibrium is not the desired situation in atomization may be in cooling towers and other applications where a steady film thickness is desired. Since there are no droplets near the entrance of the pipe or injector, mass deposition is zero. As atomization occurs the number of droplets in the flow increases causing the mass deposition to increase until equilibrium is achieved some distance from the inlet. Recent work has been more focused on flow development near start-up and on dry-out prediction ([73, 129], for instance). Correlations for four different parameters, generally for

annular flow in pipes, will be presented: onset of atomization, film thickness, entrainment rate/fraction and droplet size.

Onset of Atomization

Several different correlations exist for the inception of atomization; onset conditions are often needed as part of correlations for other parameters. Azzopardi [44] examines several methods for predicting the onset of atomization in annular flow. For example, by assuming entrainment starts when the waves penetrate the gas boundary layer, a relation between the critical Reynolds number and the grouping $(\rho_f/\rho_g)^{0.75}(\mu_g/\mu_f)^{1.5}$ can be generated [130]. Considering the stability of the disturbance waves Asali et al. [131] and Owen and Hewitt [132] determine correlations dependent on $(\rho_f/\rho_g)^{1/2}(\mu_g/\mu_f)$. Unfortunately, none of these relations appear applicable over a wide range of conditions [44]. Instead, Azzopardi [44] suggests that the onset of entrainment is related to the Weber number and reports that $Re_{mf}(Oh)^{1/2}$ versus We_{gi}/Re_{gi} give a good indication of inception criteria. Here $Re_{mf}=m_f''d_{pipe}/\mu_f$, $Oh=\mu_f/(\sigma\rho_f d_{pipe})^{1/2}$ and $We_{gi}/Re_{gi}=Ta_{gi}=\mu_g u_{g,i}/\sigma$. Okawa et al. [42] make use of Owen and Hewitt's [132] criteria for entrainment, $Re_{mf}\geq \exp[5.8504+0.4249(\rho_f/\rho_g)^{1/2}(\mu_g/\mu_f)]$, in their decision of what experimental data should be used in correlation development. Pan and Hanratty [133] use experimental measurements of critical gas and fluid flow rates to generate a critical value for $We_{gi}^{1/2}=[d_g u_{g,c}^2(\rho_f/\rho_g)^{1/2}/\sigma]^{1/2}=40$.

Film Thickness and Friction Factor

Within the development of entrainment rates two other sets of subcorrelations are often needed: one for equilibrium and entrance entrainment fractions and one for interfacial friction and film thickness. The often-used subcorrelations for interfacial friction factor and film thickness are due to Wallis [134]. He gives the interfacial friction factor as $f_i=0.005(1+300\delta/d_{pipe})$ and calculates the film thickness by equating the friction force on the wall with that at the interface, $f_i\rho_g u_g^2=f_w\rho_f u_f^2$, and letting the wall friction factor equal $f_w=0.005$ and $u_f\approx d_{pipe}Q_f''/(4\delta_f)$. Ambrosini et al. [135] use a different correlation for the friction factor based on earlier experimental work: $f_i/f_s=1+13.8We_{gp}^{0.2}Re_{gp}^{-0.6}(\delta_g^* - 200(\rho_f/\rho_g)^{1/2})$ where $f_s=0.046Re_{gp}^{-0.2}$ and $\delta_g^*=\delta\mu_{g,i}/v_g$. Here We_{gp} and Re_{gp} are based on gas properties, gas velocity and pipe diameter. They claim this correlation should be more general than the one by Wallis [134]. No comparison of the two are made within Ambrosini et al.'s [135] work, however, and their inclusion of coalescence in their formulation of entrainment rates make comparisons less than conclusive. They also offer a different film thickness correlation, $\delta u_{f,i}/v_f=cRe_{mf}^n$. The liquid velocity at the interface is calculated based on a characteristic shear related to the wall and interfacial shear stresses derived from momentum balances for the vertically upward flow. Two different behaviors are found. For low Reynolds numbers the constants proposed by Asali et al. [131], $\delta u_{f,i}/v_f=0.34Re_{mf}^{0.6}$, works well, but $Re_{mf}>1000$ results are predicted by $\delta u_{f,i}/v_f=0.0512Re_{mf}^{0.875}$ where the constants are based on the one-seventh power law proposed by Kosky [136]. Again, no comparisons with the results of Wallis are presented.

Entrainment Rate/Fraction

The bulk of correlations involve the prediction of entrainment rates or entrainment fractions. In the recent literature there appear to be two main approaches to correlation development. One is due to Dallman et al. [137] where a linear correlation between atomization rate and liquid mass flow is made; the other is related to work by Tatterson et al. [138] where it

is assumed that a competition between interfacial friction (shear) and surface tension forces controls atomization. Different developments slightly modify these main approaches and differ in how unknowns are calculated; consequently, differing correlations are obtained.

As noted above, a subcorrelation is often needed for the entrance entrainment fraction. The most commonly used development is due to Ishii and Mishima [139] and is coupled with the idea that the droplet deposition and entrainment rates are equal at equilibrium. In this subcorrelation the entrainment fraction is given as $E_\infty = \tanh[7.25 \times 10^{-7} (We_g (\Delta\rho/\rho_g)^{1/3})^{1.25} Re_{Qf}^{0.25}]$; $We_g = \rho_g u^2 d_H / \sigma$ and $Re_{Qf} = \rho_f Q_f'' d_H / \mu_f$. Work by Lopez de Bertodano et al. [73], Ebner et al. [140] and Okawa et al. [42] find that this correlation has a very limited range of applicability and does not fit the data they are studying. Lopez de Bertodano et al. [73] derive a different relation for vertical annular flow, as discussed below. Ebner et al. [140], who studied flat-bottomed, horizontal oil films, recommend a different correlation for entrainment fraction, $E = 1.042 \times 10^{-7} We_g^{1.2} Re_{Qh}^{0.4} (L/d_h)^{0.8} [1 + 2.061 \times 10^{-4} Re_{Qh}^2 / (We_g Fr_f)]^{2.25}$ where $Fr_f = Q_f''^2 / (h_{\text{pipe}} g \sin \theta)$ and $Re_{Qh} = \rho_f Q_f'' h_{\text{pipe}} / \mu_f$. This latter correlation has only been applied to their data, so its range of applicability is not fully known. Additionally, this correlation is difficult to apply because the wavelength is often unknown.

Refocusing on equilibrium entrainment rates, Lopez de Bertodano et al. [73] (hereafter LdB) and Pan and Hanratty [133, 141] (hereafter P&H) use the Dallman correlation as a starting point for developing their correlations. Both follow similar paths and replace the entrainment coefficient, k_{en} , with k_{en}'/σ to account for surface tension effects. This substitution is based on scaling arising from the idea that entrainment is linked to Kelvin-Helmholtz instabilities. The scaling appears to be correct for LdB's comparison of Freon and water-air data in vertically upward annular flow. LdB give Dallman's correlation as $m_{en}'' = k_{en} (m_f - m_{f,c}/P) u_g^2 (\rho_g \rho_f)^{1/2}$ and eventually nondimensionalize it to arrive at their final correlation $m_{en}'' d_{\text{pipe}} / \mu_f = (k_{en}'/4) (Re_p - Re_{p,c}) We_{gp} (\rho_f / \rho_g)^{1/2}$ with $Re_p = m_f / (\mu_f P)$ and $k_{en}' = 2 \times 10^{-7}$. P&H also find the surface tension scaling to be correct for vertical and horizontal annular flow. They report Dallman's correlation slightly differently as $m_{en}'' = k_{en} (m_f - m_{f,c}/P) u_g^{n+1} (\rho_g \rho_f)^{1/2}$ noting that $n=1$ was originally suggested but that other workers have successfully used $n=0$ for lower entrainment fractions and small pipes. For vertical flow they replace u_g^2 with $(u_g - u_{g,c})^2$ to properly account for the onset of atomization, but note that for horizontal flow this substitution is not proper because the critical condition varies along the circumference of the pipe. Initially, they introduce a parameter to account for this circumferential variation, but eventually choose a formulation that allows their vertical and horizontal correlations to vary only by an additional concentration term in the denominator of the horizontal flow correlation. Instead of calculating an entrainment rate, P&H correlate an entrainment fraction, E , so that $(E/E_m) / [1 - (E/E_m)] = k_{en}' d_{\text{pipe}} (u_g - u_{g,c})^2 u_g (v_d/u_g) (\rho_g \rho_f)^{1/2} / (4 k_d \sigma \chi)$ with $E_m = 1 - (m_{f,c}/m_f)$. For vertical flow $\chi = 1$; χ is a droplet concentration ratio for horizontal flow. In order to use these results, however, $u_{g,c}$, k_d and, for horizontal flow, the concentration parameter are needed. P&H determine $u_{g,c}$ from experimental data. The other two values take on assumed dependences. For vertical flow satisfactory results are found by letting $k_d / (v_d/u_g) = u_g$, which results in E/E_m being proportional to a modified Weber number $d_{\text{pipe}} (u_g - u_{g,c})^2 (\rho_g \rho_f)^{1/2} / \sigma$. A more complex correlation assuming k_d is proportional to the root-mean-square velocity of the droplets is also tried. This more complex result is more accurate for large pipe diameters, but the same equation does not predict small pipe results very well. For horizontal flow P&H follow a path similar to their vertical flow correlations where a simple form for $k_d \chi$ is introduced. They set $k_d \chi$ equal to the terminal velocity of a droplet, $u_t^2 = 4 d_d g \rho_f / (3 C_D \rho_g)$ with C_D proportional to $Re_{tg} = d_d u_t \rho_g / \mu_g$ raised to some

power, m . Tatterson et al.'s [138] work is then used to estimate droplet size: $(\rho_g u_g^2 SMD/\sigma)(SMD/d_{pipe})=0.0091$ and $(\rho_g u_g^2 SMD/\sigma)(SMD/\lambda)=0.14$ with $\lambda=(\rho g/\sigma)^{-1/2}$ as given by Azzopardi [142]. More complex relations for $k_d \chi$ are considered as well but are not presented here due to their complexity. P&H also present a very simplified approximation for entrainment fraction in horizontal flows by assuming $d_d \sim 1/u_g$ and that $u_{g,c}$ is defined as that for which $E/E_m/(1-E/E_m)$ is small. With these simplifications the correlation becomes $E/E_m/(1-E/E_m)=0.05(u_g/u_{g,c})^{3+(1+m)/(2-m)}$ where m is determined from the chosen drag coefficient relation ($C_D \propto Re_{tg}^{-m}$).

A second approach to calculating the entrainment rate is used by Ambrosini et al. [135] and Okawa et al. [42, 143] (hereafter Okawa) based on Tatterson's idea of atomization through stripping. Ambrosini et al. [135] include the effects of coalescence; consequently, because the focus of this paper is primary atomization, the details of their correlation are not given. Okawa [42, 143] develop a correlation based on the ratio of friction to surface tension forces, i.e. the dimensionless group $f_i \rho_g Q_g^{-2} \delta_f/\sigma$. As mentioned above, they used Wallis' [134] correlation for the interfacial friction factor and film thickness. In their earlier work [143] they account for the inertia of the core droplets resulting in an entrainment rate equation $m_{en}'' = k_{en} \rho (f_i \rho_g Q_g^{-2} \delta_f/\sigma) (\rho_f/\rho_g)^n$; in their later work [42] this equation is slightly altered to $m_{en}'' \sim k_{en} \rho (f_i \rho_g Q_g^{-2} \delta_f/\sigma)^n$. Further development of the earlier correlation is not detailed here since the latter work is considered to supersede it. Okawa [42] start with the assumption of equilibrium, so that $m_{en}'' = m_d'' = k_d C_d$ and they determine k_d from their experiments based on their earlier form $k_d = c(\sigma/d_d C_d)^{1/2}$ [143]. They conclude that their correlation does a better job of collapsing the data than many earlier correlations, but overestimates it, likely due to some dependence of k_d on length. Consequently, they let $k_d = k_{d0} f(L)$ and from their experimental data find $k_d = 0.040(\sigma/d_d C_d)^{1/2}$. They plot $k_d C_d / \rho_f$ versus their dimensionless number, $f_i \rho_g Q_g^{-2} \delta_f/\sigma$, and find a good fit for $k_d C_d / \rho_f = 5.1 \times 10^{-4} (f_i \rho_g Q_g^{-2} \delta_f/\sigma)^{1/2}$. Assuming equilibrium, then, $m_{en}'' = 5.1 \times 10^{-4} \rho (f_i \rho_g Q_g^{-2} \delta_f/\sigma)^{1/2} / f(L)$; they do not determine $f(L)$.

Droplet Diameter

Correlations for droplet diameter can also be found in the literature. Here a brief sampling from the film literature is given. Azzopardi [44] presents the assumptions and ideas on which several of these correlations are based. The idea that entrainment is governed by Kelvin-Helmholtz waves leads Tatterson et al. [138] to a correlation relating nondimensional droplet diameter to the $We^{1/2}$ (based on gas friction velocity, gas density and film thickness). Pan and Hanratty [141] use this idea to generate a correlation for droplet diameter, which is needed to determine the terminal velocities of the droplets. Their findings appear above. Andreussi et al. [144] give a correlation with two terms, one proportional to $u_g^{-2.0}$ and the other to $\tau_f^{1/2}$. Earlier work by Azzopardi et al. [145] developed a correlation assuming that secondary droplet breakup was important. For practical purposes, secondary breakup is important and must be considered to accurately predict droplet diameters in the system, but this paper focuses on primary atomization. Li et al. [75] try a correlation of the form $We_{gd} = c Ta_{gd} + We_{gd0}$, but find that c depends on the Re_{gd} of the flow. (These nondimensional values are based on gas properties, droplet diameter and relative velocity.) Consequently, they conclude that the nondimensional droplet diameter should be a function of Weber number only.

Datasets

Clearly experimental datasets are important for improving the range of applicability of correlations and for developing new ones in addition to their importance in validating new theories and numerical simulations. Unfortunately, few data at pressures and conditions relevant to rocket injectors exist. This paragraph reviews previously cited references which contain data or tables of papers from which further data may be obtained. Most of the work is for vertically upward annular flow. Ambrosini [135] lists several sources of data in this flow configuration. Lopez de Bertodano et al. [73] present a table of experimentally determined entrainment rates and fractions for Freon-113 liquid and vapor and for water-air. Wolf et al. [129] also present experimental results for vertically upward annular flow. Film thickness, wave frequency and speed, wall shear stress and pressure drop are given at a variety of locations along the test section. They used water and air. Okawa et al. [42] give a list of nineteen different datasets for equilibrium entrainment in annular flow with pipe dimensions, pressure ranges and entrainment fraction ranges. They also give data from their vertically upward annular flow experiments in tabular form listing pressures, gas and liquid mass fluxes and equilibrium entrainment fraction. Pan and Hanratty [133] give a brief list of experimental data available in the literature and a table containing some selected data from these experiments. Horizontal annular flow data are given in another paper by Pan and Hanratty [141] which lists some select experimental data for entrainment fraction at various gas velocities in horizontal annular flow. They also present some data in tabular form. More generally, Azzopardi [44] lists a series of twenty-nine datasets available in the literature describing annular flow in various orientations.

A few papers also deal with stratified flows either flat or in pipes. Lioumbas et al. [50] give film thicknesses, wave speeds and frequencies for stratified water-air flow in slightly inclined pipes. Ebner et al. [140] presents graphs of data for oil-air flows in an inclined rectangular duct. The flows of both Ebner et al. and Lioumbas et al. are shear driven. Datasets for turbulent films in quiescent atmospheres are also available. Dai et al. [2] present graphs for exterior annular turbulent water films. Meanwhile, Sarpkaya and Merrill [48] print graphs of flat turbulent water film data.

V. Conclusions

Atomization is a complex process that occurs over a wide range of geometries and conditions. A review of the current state of understanding of the mechanisms involved has been given. As evidenced above there are many possible drivers and paths leading to the atomization of a film. Clearly, different conditions may drastically alter the atomization mechanisms involved. As mentioned at the outset of this paper, the main motivation for this review is a basis for understanding a unique class of rocket injectors where atomization progresses from a film. Most injectors rely on the atomization of sheets or jets; consequently, little experimental and theoretical work has focused on film atomization particularly under the conditions likely in rocket injectors—high pressures, for example. Film atomization is important in other processes, however, and various atomization mechanisms have been studied for these other systems. Of the mechanisms suggested only a few have corroborating experimental evidence in the film configuration—droplets hitting films and collapsing ligaments splash creating smaller droplets [107], bubbles rupturing in oceanic flows cause sprays of droplets, wave breaking also creates sprays of droplets [89], protrusions caused by liquid turbulence break up into droplets [48], bag breakup has been observed in annular flows [44] and strong evidence of stripping exists [44]. Some support for hydrodynamic instability work also exists, although the driving forces and mechanisms for generating droplets from these instabilities remain unclear. The other

mechanisms suggested here remain to be verified. Vastly different operating conditions, disparities in emphasis and diverse figures of merit hamper the application of the existing understanding of atomization in these other configurations, primarily cooling tubes, to rocket injectors, however. For these reasons atomization mechanisms have been stressed over correlations. Different mechanisms may be important in different situations, but the understanding of the mechanism itself is applicable over a wide range of conditions.

To determine possible mechanisms and similarities between films and the better understood geometries of jet and sheet, the atomization regimes of each configuration were presented. Throughout the literature, film atomization is generally considered to take place in a Surface Breakup mode. Ribbon Forming, analogous to Sheet Pinching and Rayleigh Breakup of sheets and jets, or a Perforated mode of breakup is considered possible, though generally unlikely. A Prompt Atomization mode where the film disintegrates upon exit from a nozzle is also considered, but evidence suggests that this mode may not truly exist.

Atomization via the Surface Breakup, Ribbon Forming and Perforated regimes can be divided into two subprocesses: disturbance formation and disturbance break down. Means of disturbance formation include liquid turbulence, hydrodynamic instabilities, gas-phase vortices, pressure fluctuations, various perforation causes and diverse bubble creation mechanisms. Disturbances fit into one of four classes: waves, ligaments, perforations or bubbles. Breakdown mechanisms include wave breaking, "bag" breakup, Rayleigh breakup, aerodynamic stripping, detachment of the disturbance at its base, fragile shattering, bubble rupture and splashing. Possible prompt atomization mechanisms are also considered, although this breakup mode is judged to be less likely in films than in sheets/jets.

Attempts have been made to offer quantitative theories when available in the literature. The theories often require a better knowledge of flow and film parameters, such as velocity profiles or film thickness, than is currently available. Additionally, many of the theories require simplifications which may not be applicable at the time of atomization (e.g., linear stability theories assume the disturbance is small). To overcome some of these difficulties empirical correlations have been developed either for the entire process or for some important parameter whose knowledge is crucial in applying a particular theory. Unfortunately, these correlations have a limited range of applicability, one which is generally outside of the operating range of rocket injectors. Key nondimensional parameters which will aid in future studies have been identified from the theories and correlations, however.

One must remember that the breakdown of a disturbance only occurs if and when that projection reaches a critical size and remains at that size (or greater) for a sufficient time for the breakdown process to progress past a critical point. Consequently, not all disturbed films will undergo atomization, especially since the liquid generally spends a limited time within the atomizer. These limitations demonstrate the need to predict not only the physics of disturbance initiation, growth and breakup, but the time and distances involved via predictions of growth rates, decay rates and critical sizes of disturbances and the time for breakdown of the disturbances. A final complication to predicting film atomization is addressed only tangentially here: knowing which of the atomization mechanisms is occurring under a given set of conditions. Clearly, there are sets of conditions for which some mechanisms cannot apply; in general, however, more than one mechanism will be possible under the operating conditions. Multiple mechanisms may occur simultaneously and aid or hamper one another. Further experimental investigations will be needed to address this issue and generate a regime map(s) as available for jets.

Acknowledgements

Douglas Talley and Stephen Danczyk of AFRL have been instrumental in the preparation of this manuscript.

Nomenclature

a =Acceleration
 A =Area
 b =Distance
 Bo =Bond number
 c =Constant
 C =Concentration
 C_D =Drag coefficient
 d =Diameter
 d_f =Integral diameter= $d_H/8$
 E =Entrainment fraction
 f =Generic function
 f_i =Friction factor at the interface
 f_s =Friction factor at smooth interface
 f_w =Friction factor at the wall
 F =Force
 Fr =Froude number
 g =Acceleration of gravity
 h =Height
 k =Wave number
 k_d =Deposition coefficient
 k_{en} =Entrainment coefficient
 K =Sommerfeld parameter
 L =Length
 La =Laplace number
 m =Mass flow rate
 n =Formation rate
 N =Number
 Oh =Ohnesorge number
 p =Pressure
 P =Perimeter
 Q =Volume flow rate
 R =Radius
 Re =Reynolds number
 s_c =Normalized momentum
 SMD =Sauter Mean Diameter
 t =Time
 Ta =Taylor number
 u =Gas velocity
 v =Liquid velocity
 V =Volume
 VF =Volume fraction
 W =Width
 We =Weber number
 α =Impact angle
 β =Sheltering parameter

δ =Thickness
 ϕ =Rivulet profile
 λ =Wavelength
 ν =Kinematic viscosity
 θ =Angle of inclination
 ρ =Density
 σ =Surface tension
 τ =Shear stress

Subscripts

b =Breakup
 B =Bubble
 BL =Boundary layer
 c =Critical
 cen =Centripetal
 cr =Created
 cs =Cross section
 cv =Control volume
 d =Droplet
 dp =dry patch
 dry =Dry out
 e =Eddy
 en =Entrained
 f =Liquid
 Fd =Film droplets
 g =Gas
 gf =Gas-liquid
 $grav$ =Gravity
 H =Hydraulic
 i =Interface
 img =Imaginary
 in =Initial
 j =Jet
 Jd =Jet droplets
 lig =Ligament
 m =Mean or average
 min =Minimum
 R =Rayleigh
 r =Reference
 rel =Relative
 rms =Root-mean-square
 s =Sheet
 t =Terminal
 $vert$ =Vertical
 w =Wave
 σ =Surface tension

References

1. I. S. Carvalho, M. V. Heitor and D. Santos, Liquid Film Disintegration Regimes and Proposed Correlations, *International Journal of Multiphase Flow*, vol. 28, no. 5, pp. 773-789, 2002.
2. Z. Dai, W. H. Chou and G. M. Faeth, Drop Formation Due to Turbulent Primary Breakup at the Free Surface of Plane Liquid Wall Jets, *Physics of Fluids*, vol. 10, no. 5, pp. 1147-1157, 1998.
3. A. H. Lefebvre, Energy Considerations in Twin-Fluid Atomization, *Journal of Engineering for Gas Turbines and Power-Transactions of the ASME*, vol. 144, no. 1, pp. 89-96, 1992.
4. I. S. Carvalho and M. V. Heitor, Liquid Film Break-up in a Mode of a Prefilming Airblast Nozzle, *Experiments in Fluids*, vol. 24, no. 5-6, pp. 408-415, 1998.
5. A. H. Lefebvre, *Atomization and Sprays*, Hemisphere Press, New York, 1989.
6. N. Chigier, Breakup of Liquid Sheets and Jets, AIAA-1999-3640, 30th AIAA Fluid Dynamics Conference, Norfolk, VA, June 28-July 1, 1999.
7. J. Shen and X. Li, Instability of an Annular Viscous Liquid Jet, *Acta Mechanica*, vol. 114, no. 1-4, pp. 167-183, 1996.
8. R. K. Cohn, P. Strakey, J. A. Muss, C. W. Johnson, R. W. Bates and D. G. Talley, Swirl Coaxial Injector Development, AIAA-2003-0125, 41st Aerospace Sciences Meeting and Exhibit, Reno, NV, January 6-9, 2003.
9. M. D. A. Lightfoot, S. A. Danczyk and D. G. Talley, Atomization in Gas-Centered Swirl-Coaxial Injectors, 19th Annual Conference on Liquid Atomization and Spray Systems, Toronto, ON, May 23-26, 2006.
10. P. Strakey, R. K. Cohn and D. G. Talley, The Development of a Methodology to Scale between Cold-Flow and Hot-Fire Evaluations of Gas-Centered Swirl Coaxial Injectors, 52nd JANNAF Propulsion Meeting, Las Vegas, NV, May 10-14, 2004.
11. S. P. Lin and R. D. Reitz, Drop and Spray Formation from a Liquid Jet, *Annual Review of Fluid Mechanics*, vol. 30, pp. 85-105, 1998.
12. J. C. Lasheras and E. J. Hopfinger, Liquid Jet Instability and Atomization in a Coaxial Gas Stream, *Annual Review of Fluid Mechanics*, vol. 32, pp. 275+, 2000.
13. R. J. Margason, Fifty Years of Jet in Crossflow Research, AGARD CP-534, AGARD Symposium on a Jet in Cross Flow, Winchester, UK, 1993.

14. K. A. Sallam, Z. Dai and G. M. Faeth, Turbulent Primary Breakup of Round and Plane Liquid Jets in Still Air, AIAA-2002-1115, 40th AIAA Aerospace Sciences Meeting and Exhibit, Reno, NV, January 14-17, 2002.
15. R. D. Reitz and F. V. Bracco, Mechanism of Atomization of a Liquid Jet, *Physics of Fluids*, vol. 25, no. 10, pp. 1730-1742, 1982.
16. S. P. Lin and J. N. Chen, Role Played by the Interfacial Shear in the Instability Mechanism of a Viscous Liquid Jet Surrounded by a Viscous Gas in a Pipe, *Journal of Fluid Mechanics*, vol. 376, pp. 37-51, 1998.
17. K. A. Sallam, Z. Dai and G. M. Faeth, Liquid Breakup at the Surface of Turbulent Round Liquid Jets in Still Gases, *International Journal of Multiphase Flow*, vol. 28, no. 3, pp. 427-449, 2002.
18. G. M. Faeth, Liquid Atomization in Multiphase Flows: A Review, AIAA-1999-3639, 30th AIAA Fluid Dynamics Conference, Norfolk, VA, June 28-July 1, 1999.
19. L. A. Jurman and M. J. McCready, Study of Waves on Thin Liquid-Films Sheared by Turbulent Gas-Flows, *Physics of Fluids A-Fluid Dynamics*, vol. 1, no. 3, pp. 522-536, 1989.
20. Y. Liao, A. T. Sakman, S. M. Jeng and M. A. Benjamin, A Comprehensive Model to Predict Simplex Atomizer Performance, *Journal of Engineering for Gas Turbines and Power-Transactions of the ASME*, vol. 121, no. 2, pp. 285-294, 1999.
21. P. K. Wu, L. P. Hsiang and G. M. Faeth, Aerodynamic Effects on Primary and Secondary Spray Breakup, *Progress in Astronautics and Aeronautics*, vol. 169, pp. 247-279, 1995.
22. G. M. Faeth, L. P. Hsiang and P. K. Wu, Structure and Breakup Properties of Sprays, *International Journal of Multiphase Flow*, vol. 21, no. Supplement, pp. 99-127, 1995.
23. K. A. Sallam and G. M. Faeth, Surface Properties During Primary Breakup of Turbulent Liquid Jets in Still Air, *AIAA Journal*, vol. 41, no. 8, pp. 1514-1524, 2003.
24. W. A. Sirignano and C. Mehring, Review of Theory of Distortion and Disintegration of Liquid Streams, *Progress in Energy and Combustion Science*, vol. 26, no. 4-6, pp. 609-655, 2000.
25. H. Fu, X. Li, L. A. Prociw and T. C. J. Hu, Experimental Investigation on the Breakup of Annular Liquid Sheets in Two Co-Flowing Airstreams, AIAA 2003-5944, 1st International Energy Conversion Engineering Conference, Portsmouth, VA, August 17-21, 2003.
26. Y. Liao, S. M. Jeng, M. A. Jog and M. A. Benjamin, Advanced Sub-Model for Airblast Atomizers, *Journal of Propulsion and Power*, vol. 17, no. 2, pp. 411-417, 2001.

27. Y. Liao, S. M. Jeng, M. A. Jog and M. A. Benjamin, On the Mechanism of Pressure-Swirl Airblast Atomization, AIAA-2001-3571, 37th AIAA/ASME/SAE/ASEE Joint Propulsion Conference and Exhibit, Salt Lake City, UT, July 8-11, 2001.
28. R. P. Fraser, P. Eisenklam, N. Dombrowski and D. Hasson, Drop Formation from Rapidly Moving Liquid Sheets, *AICHE Journal*, vol. 8, no. 5, pp. 672-680, 1962.
29. M. Adzic, I. S. Carvalho and M. V. Heitoyr, Visualization of the Disintegration of an Annular Liquid Sheet in a Coaxial Airblast Injector at Low Atomising Air Velocities, *Optical Diagnostics in Engineering*, vol. 5, no. 1, pp. 27-38, 2001.
30. Y. Khavkin, *Theory and Practice of Swirl Atomizers*, Taylor and Francis, New York, 2004.
31. N. Dombrowski and W. R. Johns, The Aerodynamic Instability and Disintegration of Viscous Liquid Sheets, *Chemical Engineering Science*, vol. 18, no. 3, pp. 203-214, 1963.
32. D. P. Schmidt, I. Nouar, P. K. Senecal, J. Hoffman, C. J. Rutland, J. Martin and R. D. Reitz, Pressure-Swirl Atomization in the near Field, SAE Technical Paper Series, 1999-01-0496, 1999.
33. R. H. Rangel and W. A. Sirignano, The Linear and Nonlinear Shear Instability of a Fluid Sheet, *Physics of Fluids A-Fluid Dynamics*, vol. 3, no. 10, pp. 2392-2400, 1991.
34. W. W. Hagerty and J. F. Shea, A Study of the Stability of Plane Fluid Sheets, *Journal of Applied Mechanics*, vol. 22, no. 4, pp. 509-514, 1955.
35. B. E. Stapper, W. A. Sowa and G. S. Samuelsen, An Experimental-Study of the Effects of Liquid Properties on the Breakup of a 2-Dimensional Liquid Sheet, *Journal of Engineering for Gas Turbines and Power-Transactions of the ASME*, vol. 114, no. 1, pp. 39-45, 1992.
36. C. Clanet and E. Villermaux, Life of a Smooth Liquid Sheet, *Journal of Fluid Mechanics*, vol. 462, pp. 307-340, 2002.
37. K. Jung, B. Lim, T. Khil and Y. Yoon, Breakup Characteristics of Laminar and Turbulent Liquid Sheets Formed by Impinging Jets in High Pressure Environments, AIAA-2004-3526, 40th AIAA/ASME/SAE/ASEE Joint Propulsion Conference and Exhibit, Fort Lauderdale, FL, July 11-14, 2004.
38. A. Ghafourian, S. Mahalingam, H. Dindi and J. W. Daily, A Review of Atomization in Liquid Rocket Engines, AIAA 91-0283, 29th Aerospace Sciences Meeting, Reno, NV, January 7-10, 1991.

39. W. E. Anderson, H. M. Ryan and R. J. Santoro, Impinging Jet Injector Atomization, *Progress in Astronautics and Aeronautics*, vol. 169, pp. 215-246, 1995.
40. E. Villermaux and C. Clanet, Life of a Flapping Liquid Sheet, *Journal of Fluid Mechanics*, vol. 462, pp. 341-363, 2002.
41. S. D. Sovani, P. E. Sojka and A. H. Lefebvre, Effervescent Atomization, *Progress in Energy and Combustion Science*, vol. 27, no. 4, pp. 483-521, 2001.
42. T. Okawa, A. Kotani and I. Kataoka, Experiments for Liquid Phase Mass Transfer Rate in Annular Regime for a Small Vertical Tube, *International Journal of Heat and Mass Transfer*, vol. 48, no. 3-4, pp. 585-598, 2005.
43. M. J. Holowach, L. E. Hochreiter and F. B. Cheung, A Model for Droplet Entrainment in Heated Annular Flow, *International Journal of Heat and Fluid Flow*, vol. 23, no. 6, pp. 807-822, 2002.
44. B. J. Azzopardi, Drops in Annular Two-Phase Flow, *International Journal of Multiphase Flow*, vol. 23, no. Supplement, pp. 1-53, 1997.
45. M. S. El-Genk and H. H. Saber, Minimum Thickness of a Flowing Down Liquid Film on a Vertical Surface, *International Journal of Heat and Mass Transfer*, vol. 44, no. 15, pp. 2809-2825, 2001.
46. P. Yecko and M. Rossi, Transient Growth and Instability in Rotating Boundary Layers, *Physics of Fluids*, vol. 16, no. 7, pp. 2322-2335, 2004.
47. W. O. H. Mayer, Coaxial Atomization of a Round Liquid Jet in a High Speed Gas Stream: A Phenomenological Study, *Experiments in Fluids*, vol. 16, no. 6, pp. 401-410, 1994.
48. T. Sarpkaya and C. F. Merrill, Spray Generation from Turbulent Plane Water Wall Jets Discharging into Quiescent Air, *AIAA Journal*, vol. 39, no. 7, pp. 1217-1229, 2001.
49. T. Sarpkaya, Characterization of the Free Surface Structures on High-Speed Liquid Jets, 8th ICCLASS, Pasadena, CA, July 16-20, 2000.
50. J. S. Lioumbas, S. V. Paras and A. J. Karabelas, Co-Current Stratified Gas-Liquid Downflow--Influence of the Liquid Flow Field on Interfacial Structure, *International Journal of Multiphase Flow*, vol. 31, no. 8, pp. 869-896, 2005.
51. S. P. Lin and Z. L. Wang, Three Types of Linear Theories for Atomizing Liquids, 19th Annual Conference on Liquid Atomization and Spray Systems, Toronto, ON, May 23-26, 2006.

52. P. Yecko, Breakup Growth in Primary Atomization: Three-Dimensionality, Transient Amplification and Non-Parallel Flow Effects, 16th ILASS Americas, Monterey, CA, May 18-21, 2003.
53. P. Yecko, Optimal Breakup Structure and Development on a Sheared Interface, 17th ILASS Americas, Arlington, VA, May 16-19, 2004.
54. P. Yecko and S. Zaleski, Transient Growth in Two-Phase Mixing Layers, *Journal of Fluid Mechanics*, vol. 528, pp. 43-52, 2005.
55. A. Lozano, A. Garcia-Olivares and C. Dopazo, The Instability Growth Leading to a Liquid Sheet Breakup, *Physics of Fluids*, vol. 10, no. 9, pp. 2188-2197, 1998.
56. C. Mehring and W. A. Sirignano, Nonlinear Capillary Waves on Swirling, Axisymmetric Free Liquid Films, *International Journal of Multiphase Flow*, vol. 27, no. 10, pp. 1707-1734, 2001.
57. H. B. Squire, Investigation of the Instability of a Moving Liquid Film, *British Journal of Applied Physics*, vol. 4, pp. 167-169, 1953.
58. J. L. York, H. E. Stubbs and M. R. Tek, Mechanism of Disintegration of Liquid Sheets, *Transactions of the ASME*, vol. 75, pp. 1279-1286, 1953.
59. Z.-N. Wu, Most Unstable Waves of a Stagnant Planar Liquid Film Blown by a High Speed Viscous Gas with a Blasius Velocity Profile, *Acta Mechanica*, vol. 149, pp. 69-83, 2001.
60. X. G. Li and R. S. Tankin, On the Temporal Instability of a 2-Dimensional Viscous-Liquid Sheet, *Journal of Fluid Mechanics*, vol. 226, pp. 425-443, 1991.
61. J. W. Miles, On the Generation of Surface Waves by Shear Flow, Part 4, *Journal of Fluid Mechanics*, vol. 13, pp. 433-448, 1962.
62. J. W. Miles, The Hydrodynamic Stability of a Thin Film of Liquid in Uniform Shearing Motion, *Journal of Fluid Mechanics*, vol. 8, pp. 593-611, 1960.
63. A. D. D. Craik, Wind Generated Waves in Thin Films, *Journal of Fluid Mechanics*, vol. 26, pp. 369-392, 1966.
64. T. B. Benjamin, The Threefold Classification of Unstable Disturbances in Flexible Surfaces Bounding Inviscid Flows, *Journal of Fluid Mechanics*, vol. 16, no. 3, pp. 436-450, 1963.
65. P. A. M. Boomkamp and R. H. M. Miesen, Classification of Instabilities in Parallel Two-Phase Flow, *International Journal of Multiphase Flow*, vol. 22, no. Supplement, pp. 67-88, 1996.

66. S. Ozgen, G. Degrez and G. S. R. Sarma, Two-Fluid Boundary Layer Stability, *Physics of Fluids*, vol. 10, no. 11, pp. 2746-2757, 1998.
67. P. Yecko, S. Zaleski and J. M. Fullana, Viscous Modes in Two-Phase Mixing Layers, *Physics of Fluids*, vol. 14, no. 12, pp. 4115-4122, 2002.
68. G. Hauke, C. Dopazo, A. Lozano, F. Barreras and A. H. Hernandez, Linear Stability Analysis of a Viscous Liquid Sheet in a High-Speed Viscous Gas, *Flow Turbulence and Combustion*, vol. 67, no. 3, pp. 235-265, 2001.
69. S. Ostrach and A. Koestel, Film Instabilities in Two-Phase Flows, *AICHE Journal*, vol. 11, no. 2, pp. 294-303, 1965.
70. P. G. Drazin and W. H. Reid, *Hydrodynamic Stabilities*, Cambridge University Press, Cambridge, 1984.
71. G. Lavergne, P. Trichet, P. Hebrard and Y. Biscos, Liquid Sheet Disintegration and Atomization Process on a Simplified Airblast Atomizer, *Journal of Engineering for Gas Turbines and Power-Transactions of the ASME*, vol. 115, no. 3, pp. 461-466, 1993.
72. J. Park, K. Y. Huh, X. Li and M. Renksizbulut, Experimental Investigation on Cellular Breakup of a Planar Liquid Sheet from an Air-Blast Nozzle, *Physics of Fluids*, vol. 16, no. 3, pp. 625-632, 2004.
73. M. A. Lopez de Bertodano, A. Assad and S. G. Beus, Experiments for Entrainment Rate of Droplets in the Annular Regime, *International Journal of Multiphase Flow*, vol. 27, no. 4, pp. 685-699, 2001.
74. T. Inamura, H. Yanaoka and T. Tomoda, Prediction of Mean Droplet Size of Sprays Issued from Wall Impingement Injector, *AIAA Journal*, vol. 42, no. 3, pp. 614-621, 2004.
75. J. Li, E. Lopez-Pages, P. Yecko and S. Zaleski, Droplet Formation in Sheared Liquid-Gas Layer, *Theoretical and Computational Fluid Dynamics*, vol. submitted, pp. 2005.
76. A. Lozano and F. Barreras, Experimental Study of the Gas Flow in an Air-Blasted Liquid Sheet, *Experiments in Fluids*, vol. 31, no. 4, pp. 367-376, 2001.
77. N. Chigier and R. D. Reitz, Regimes of Jet Breakup and Breakup Mechanisms--Physical Aspects, *Progress in Astronautics and Aeronautics*, vol. 166, pp. 109-135, 1996.
78. E. Lopez-Pages, C. Dopazo and N. Fueyo, Very-near-Field Dynamics in the Injection of Two-Dimensional Gas Jets and Thin Liquid Sheets between Two Parallel High-Speed Gas Streams, *Journal of Fluid Mechanics*, vol. 515, pp. 1-31, 2004.

79. W. O. H. Mayer and R. Branam, Atomization Characteristics on the Surface of a Round Liquid Jet, *Experiments in Fluids*, vol. 36, no. 4, pp. 528-539, 2004.
80. M. Klein, Direct Numerical Simulation of a Spatially Developing Water Sheet at Moderate Reynolds Number, *International Journal of Heat and Fluid Flow*, vol. 26, no. 5, pp. 722-731, 2005.
81. V. N. Kudryavtsev, V. K. Makin and J. F. Meirink, Simplified Model of the Air Flow above Waves, *Boundary-Layer Meteorology*, vol. 100, no. 1, pp. 63-90, 2001.
82. J. Canino, S. Heister, V. Sankaran and S. Zakharov, Unsteady Response of Recessed-Post Coaxial Injectors, AIAA-2005-4297, 41st AIAA/ASME/SAE/ASEE Joint Propulsion Conference and Exhibit, Tucson, AZ, July 10-13, 2005.
83. P. Strakey and D. Talley, Rocket Injector Science, *FLUENT News*, vol. Fall, pp. 14-15, 2004.
84. V. G. Bazarov, Non-Linear Interactions in Liquid-Propellant Rocket Engine Injectors, AIAA 1998-4039, 34th AIAA/ASME/SAE/ASEE Joint Propulsion Conference and Exhibit, Cleveland, OH, July 13-15, 1998.
85. A. Alajbegovic, G. Meister, D. Greif and B. Basara, Three Phase Cavitating Flows in High-Pressure Swirl Injectors, *Experimental Thermal and Fluid Science*, vol. 26, no. 6-7, pp. 677-681, 2002.
86. J. Murphy, D. Schmidt, S. P. Wang and M. L. Corradini, Multi-Dimensional Modeling of Multiphase Flow Physics: High-Speed Nozzle and Jet Flows - a Case Study, *Nuclear Engineering and Design*, vol. 204, no. 1-3, pp. 177-190, 2001.
87. M. X. Yuan and U. H. Schnerr, Numerical Simulation of Two-Phase Flow in Injection Nozzles: Interaction of Cavitation and External Jet Formation, *Journal of Fluids Engineering-Transactions of the ASME*, vol. 125, no. 6, pp. 963-969, 2003.
88. K. Heukelbach and C. Tropea, Influence of the Inner Flowfield of Flat Fan Pressure Atomizers on the Disintegration of the Liquid Sheet, ILASS-Europe, Zurich, Switzerland, September 2-6, 2001.
89. G. Chen, C. Kharif, S. Zaleski and J. Li, Two-Dimensional Navier-Stokes Simulation of Breaking Waves, *Physics of Fluids*, vol. 11, no. 1, pp. 121-133, 1999.
90. G. B. Deane and M. D. Stokes, Scale Dependence of Bubble Creation Mechanisms in Breaking Waves, *Nature*, vol. 418, no. 6900, pp. 839-844, 2002.
91. D. J. Rodriguez and T. A. Shedd, Entrainment of Gas in the Liquid Film of Horizontal, Annular, Two-Phase Flow, *International Journal of Multiphase Flow*, vol. 30, no. 6, pp. 565-583, 2004.

92. M. Rein, Turbulent Open-Channel Flows: Drop-Generation and Self-Aeration - Closure, *Journal of Hydraulic Engineering-ASCE*, vol. 125, no. 6, pp. 670-670, 1999.
93. D. E. Woodmansee and T. J. Hanratty, Mechanism for the Removal of Droplets from a Liquid Surface by a Parallel Air Flow, *Chemical Engineering Science*, vol. 24, no. 2, pp. 299-307, 1969.
94. D. G. Penn, M. L. de Bertodano, P. S. Lykoudis and S. G. Beus, Dry Patch Stability of Shear Driven Liquid Films, *Journal of Fluids Engineering-Transactions of the ASME*, vol. 123, no. 4, pp. 857-862, 2001.
95. Y. Y. Zhao, Analysis of Flow Development in Centrifugal Atomization: Part II. Disintegration of a Non-Fully Spreading Melt, *Modeling and Simulation in Materials Science and Engineering*, vol. 12, no. 5, pp. 973-983, 2004.
96. N. S. Wilkes, B. J. Azzopardi and C. P. Thompson, Wave Coalescence and Entrainment in Vertical Annular 2-Phase Flow, *International Journal of Multiphase Flow*, vol. 9, no. 4, pp. 383-398, 1983.
97. R. M. Roberts, H.-C. Chang and M. J. McCready, Mechanism of Atomization in a Two-Layer Couette Flow, 4th Microgravity Fluid Physics and Transport Phenomena Conference in CP-1999-208526/SUPPL1, pp. 2-5, 1998.
98. P. K. Senecal, D. P. Schmidt, I. Nouar, C. J. Rutland, R. D. Reitz and M. L. Corradini, Modeling High-Speed Viscous Liquid Sheet Atomization, *International Journal of Multiphase Flow*, vol. 25, no. 6-7, pp. 1073-1097, 1999.
99. J. H. Duncan, Spilling Breakers, *Annual Review of Fluid Mechanics*, vol. 33, pp. 519-547, 2001.
100. Y. Khavkin, Secondary Drop Breakup in Swirl Atomizers, *Atomization and Sprays*, vol. 12, no. 5-6, pp. 615-627, 2002.
101. E. Mayer, Theory of Liquid Atomization in High Velocity Gas Streams, *ARS Journal*, vol. 31, no. 12, pp. 1783-1785, 1961.
102. B. E. Gelfand, Droplet Breakup Phenomena in Flows with Velocity Lag, *Progress in Energy and Combustion Science*, vol. 22, no. 3, pp. 201-265, 1996.
103. S. C. Georgescu, J. L. Achard and E. Canot, Jet Drops Ejection in Bursting Gas Bubble Processes, *European Journal of Mechanics B-Fluids*, vol. 21, no. 2, pp. 265-280, 2002.
104. A. Gunther, S. Walchli and P. R. von Rohr, Droplet Production from Disintegrating Bubbles at Water Surfaces. Single Vs. Multiple Bubbles, *International Journal of Multiphase Flow*, vol. 29, no. 5, pp. 795-811, 2003.

105. L. Duchemin, S. Popinet, C. Josserand and S. Zaleski, Jet Formation in Bubbles Bursting at a Free Surface, *Physics of Fluids*, vol. 14, no. 9, pp. 3000-3008, 2002.
106. F. MacIntyre, Flow Patterns in Breaking Bubbles, *Journal of Geophysical Research*, vol. 77, no. 27, pp. 5211-5228, 1972.
107. K. L. Pan and C. K. Law, Dynamics of Droplet-Film Collision, AIAA-2005-0352, 43rd AIAA Aerospace Sciences Meeting and Exhibit, Reno, NV, January 10-13, 2005.
108. C. Josserand and S. Zaleski, Droplet Splashing on a Thin Liquid Film, *Physics of Fluids*, vol. 15, no. 6, pp. 1650-1657, 2003.
109. W. Samenfink, A. Elsasser, K. Dullenkopf and S. Wittig, Droplet Interaction with Shear-Driven Liquid Films: Analysis of Deposition and Secondary Droplet Characteristics, *International Journal of Heat and Fluid Flow*, vol. 20, no. 5, pp. 462-469, 1999.
110. G. Reiter, Dewetting of Thin Polymer-Films, *Physical Review Letters*, vol. 68, no. 1, pp. 75-78, 1992.
111. G. Reiter, Unstable Thin Polymer-Films - Rupture and Dewetting Processes, *Langmuir*, vol. 9, no. 5, pp. 1344-1351, 1993.
112. H. H. Saber and M. S. El-Genk, On the Breakup of a Thin Liquid Film Subject to Interfacial Shear, *Journal of Fluid Mechanics*, vol. 500, pp. 113-133, 2004.
113. F. Brochard-Wyart, P. G. Degennes, H. Hervet and C. Redon, Wetting and Slippage of Polymer Melts on Semi-Ideal Surfaces, *Langmuir*, vol. 10, no. 5, pp. 1566-1572, 1994.
114. T. Podgorski, J.-M. Flesselles and L. Limat, Curvature of a Dry Patch Boundary in a Flowing Film, *Comptes Rendus de l'Academie des Sciences, Series IV. Physics-Astrophysics*, vol. 2, no. 9, pp. 1361-1367, 2001.
115. A. M. Sterling and C. A. Sleicher, The Instability of Capillary Jets, *Journal of Fluid Mechanics*, vol. 68, no. 3, pp. 477-495, 1975.
116. R. E. Childs and N. N. Mansour, Simulation of Fundamental Atomization Mechanisms in Fuel Sprays, *Journal of Propulsion and Power*, vol. 5, no. 6, pp. 641-649, 1989.
117. Y. Khavkin, About Swirl Atomizer Mean Droplet Size, *Atomization and Sprays*, vol. 11, no. 6, pp. 757-774, 2001.
118. F. Maroteaux, D. Llory, J. F. Le Coz and C. Habchi, Liquid Film Atomization on Wall Edges - Separation Criterion and Droplets Formation Model, *Journal of Fluids Engineering-Transactions of the ASME*, vol. 124, no. 3, pp. 565-575, 2002.

119. M. A. Friedrich, H. Lan, J. A. Drallmeier and B. F. Armaly, Characterization of Shear-Driven Liquid Film Separation and Break-up at a Sharp Expanding Corner, 19th Annual Conference on Liquid Atomization and Spray Systems, Toronto, ON, May 23-26, 2006.
120. M. C. Jermy, M. Hussain and D. A. Greenhalgh, Operating Liquid-Fuel Airblast Injectors in Low-Pressure Test Rigs: Strategies for Scaling Down the Flow Conditions, *Measurement Science and Technology*, vol. 14, no. 7, pp. 1151-1158, 2003.
121. B. N. Caines, R. A. Hicks and C. W. Wilson, Influence of Sub-Atmospheric Conditions on the Performance of an Airblast Atomiser, AIAA 01-34286, 37th AIAA/ASME/SAE/ASEE Joint Propulsion Conference, Salt Lake City, UT, July 8-11, 2001.
122. Z.-N. Wu, Prediction of the Size Distribution of Secondary Ejected Droplets by Crown Splashing of Droplets Impinging on a Solid Wall, *Probabilistic Engineering Mechanics*, vol. 18, no. 3, pp. 241-249, 2003.
123. W. C. Macklin and G. J. Metaxas, Splashing of Droplets on Liquid Layers, *Journal of Applied Physics*, vol. 47, no. 9, pp. 3963-3970, 1976.
124. W. H. Henstock and T. J. Hanratty, The Interfacial Drag and Height of the Wall Layer in Annular Flows, *AICHE Journal*, vol. 22, no. 6, pp. 990-1000, 1976.
125. S. C. Lee and S. G. Bankoff, Stability of Steam Water Countercurrent Flow in an Inclined Channel: Flooding, *Journal of Heat Transfer*, vol. 105, pp. 713-718, 1983.
126. M. S. Grolmes, G. A. Lambert and H. K. Fauske, Flooding in Vertical Tubes, Multiphase Flow Systems in *AICHE Symposium Series*, vol. 38, pp. A4, 1974.
127. H. Lamb, *Hydrodynamics*, Dover Publication, New York, 1932.
128. Y.-P. Wang, M. Thiruvengadam, J. A. Drallmeier and B. F. Armaly, A Comparison of Models for Shear-Driven Liquid Film Separation around a Corner, 18th ILASS Americas, Irvine, CA, May 22-25, 2005.
129. A. Wolf, S. Jayanti and G. F. Hewitt, Flow Development in Vertical Annular Flow, *Chemical Engineering Science*, vol. 56, no. 10, pp. 3221-3235, 2001.
130. M. Ishii and M. S. Grolmes, Inception Criteria for Droplet Entrainment in Two-Phase Concurrent Flow, *AICHE Journal*, vol. 21, no. 2, pp. 308-318, 1975.
131. J. C. Asali, T. J. Hanratty and P. Andreussi, Interfacial Drag and Film Height for Vertical Annular-Flow, *AICHE Journal*, vol. 31, no. 6, pp. 895-902, 1985.
132. D. G. Owen and H. G. Hewitt, A Proposed Entrainment Correlation, UKAEA, AERE-R12279, 1986.

133. L. Pan and T. J. Hanratty, Correlation of Entrainment for Annular Flow in Vertical Pipes, *International Journal of Multiphase Flow*, vol. 28, no. 3, pp. 363-384, 2002.
134. G. B. Wallis, *One-Dimensional Two-Phase Flow*, McGraw-Hill, New York, 1969.
135. W. Ambrosini, P. Andreussi and B. J. Azzopardi, A Physically Based Correlation for Drop Size in Annular-Flow, *International Journal of Multiphase Flow*, vol. 17, no. 4, pp. 497-507, 1991.
136. P. G. Kosky, Thin Liquid Films under Simultaneous Shear and Gravity Forces, *International Journal of Heat and Mass Transfer*, vol. 14, no. 8, pp. 1220-1224, 1971.
137. J. C. Dallman, B. G. Jones and T. J. Hanratty, Interpretation of Entrainment Measurements in Annular Gas-Liquid Flow, Chemical Process and Energy Engineering System in *Two-Phase Momentum Heat and Mass Transfer*, vol. 2, pp. 681-693, 1979.
138. D. F. Tatterson, J. C. Dallman and T. J. Hanratty, Drop Size in Annular Gas-Liquid Flows, *AICHE Journal*, vol. 23, no. 1, pp. 68-75, 1977.
139. M. Ishii and K. Mishima, Droplet Entrainment Correlation in Annular 2-Phase Flow, *International Journal of Heat and Mass Transfer*, vol. 32, no. 10, pp. 1835-1846, 1989.
140. J. Ebner, M. Gerendas, O. Schafer and S. Wittig, Droplet Entrainment from a Shear-Driven Liquid Wall Film in Inclined Ducts: Experimental Study and Correlation Comparison, *Journal of Engineering for Gas Turbines and Power-Transactions of the ASME*, vol. 124, no. 4, pp. 874-880, 2002.
141. L. Pan and T. J. Hanratty, Correlation of Entrainment for Annular Flow in Horizontal Pipes, *International Journal of Multiphase Flow*, vol. 28, no. 3, pp. 385-408, 2002.
142. B. J. Azzopardi, Drop Sizes in Annular 2-Phase Flow, *Experiments in Fluids*, vol. 3, no. 1, pp. 53-59, 1985.
143. T. Okawa, T. Kitahara, K. Yoshida, T. Matsumoto and I. Kataoka, New Entrainment Rate Correlation in Annular Two-Phase Flow Applicable to Wide Range of Flow Condition, *International Journal of Heat and Mass Transfer*, vol. 45, no. 1, pp. 87-98, 2002.
144. P. Andreussi, G. Romano and S. Zanelli, Drop Size Distribution in Annular Mist Flow, First Conference on Liquid Atomisation and Spray Systems, Tokyo, Japan, August 27-31, 1978.
145. B. J. Azzopardi, Artificial Waves in Annular Two-Phase Flow, ASME Winter Annual Meeting in *Basic Mechanism in Two-Phase Flow and Heat Transfer*, vol., pp. 1-8, 1980.

Table 1**Reference**

| | Nondimensional values used/reported | | | |
|---------------------------|--|---|--|---|
| Ambrosini [135] | $Re_{mf} = m_f d_{pipe}/\mu_f$ | $Re_{gp} = \rho_g u d_{pipe}/\mu_g$ | $We_{gp} = \rho_g u^2 d_{pipe}/\sigma$ | $Oh = \mu_f/(\sigma \rho_f d_{pipe})^{1/2}$ |
| Azzopardi [44] | $Re_{mf} = m_f d_{pipe}/\mu_f$ | $Re_{gi} = \rho_g u_{g,i} d_{pipe}/\mu_g$ | $We_{gi} = \rho_g u_{g,i}^2 d_{pipe}/\sigma$ | |
| Carvalho [1] ^a | $Re_f = \rho_f v \delta_f/\mu_f$ | ρ_f/ρ_g | μ_f/μ_g | |
| Chen [89] | $Re_{grav} = \rho_f (g \lambda^3)^{1/2}/\mu_f$ | frequency δ_f/v | $\rho_g u^2/(\rho_f v^2)$ | |
| Dai [2] | $Re_{fdH} = \rho_f v_{m,i} d_H/\mu_f$ | $Bo_{grav} = \rho_g \lambda^2/\sigma$ | ρ_f/ρ_g | μ_f/μ_g |
| Ebner [140] | μ_f/μ_g | $We_{fdl} = \rho_f v_{m,i}^2 d_l/\sigma$ | $v_{m,i}/v_{rms}$ | ρ_f/ρ_g |
| Hauke [68] ^a | $Re_{Qh} = \rho_f Q_f h_{pipe}/\mu_f$ | $We_g = \rho_g u^2 d_H/\sigma$ | $Fr_f = Q_f^{1/2}/(h_{pipe} g \sin \theta)$ | $Oh_H = \mu_f/(\sigma \rho_f d_H)^{1/2}$ |
| Ishii [139] | L/d_H | | | |
| Josserand [108] | | $Re_{BL} = \rho_g u \delta_{g,BL}/\mu_g$ | $We_f/2 = \rho_f v^2 \delta_f/(2\sigma)$ | $2\delta_{g,BL}/\delta_f$ |
| Li [75] | $Re_{Qf} = \rho_f Q_f d_H/\mu_f$ | $\rho_g u^2/(\rho_f v^2)$ | | |
| Lopez de Bertodano [73] | $Re_d = \rho_f v_d d_d/\mu_f$ | $We^* = \rho_g u^2 d_H (\Delta \rho/\rho_g)^{1/3}/\sigma$ | $K = We^{1/2} Re^{1/4}$ | h_d/d_d |
| Okawa [42] | ρ_f/ρ_g | $We_d = \rho_f v_d^2 d_d/\sigma$ | | |
| Pan [141] | $Re_p = m_f/(\mu_f P)$ | $Re_g = m_f/(\mu_f P)$ | ρ_f/ρ_g | μ_f/μ_g |
| Samenfink [109] | | $We_g = \rho_g u^2 d_H/\sigma$ | | |
| Sarpkaya [48] | | $f_f \rho_g \tau_f Q_f^{1/2}/\sigma$ | | |
| Strakey [10] | | $We_D = (\rho_f \rho_g)^{1/2} d_{pipe} u^2/\sigma$ | | |
| | | $Re_d = \rho_f v_d d_d/\mu_f$ | $La = \rho_f \sigma d_d/\mu_f^2$ | τ_f/d_d |
| | | $Re_f = \rho_f v \delta_f/\mu_f$ | $We_f = \rho_f v^2 \delta_f/\sigma$ | $Fr_{fo} = v/(g \delta_f)^{1/2}$ |
| | | roughness/ δ_f | | v_{rms}/v |
| | | $Ta_{rel} = \mu_f v_{rel}/\sigma$ | v_{rel}/v | ρ_f/ρ_g |
| | | | L/δ_f | |

^afor sheets

List of Figures

Figure 1: Shown here are the three different atomization configurations and some subconfigurations thereof. The three main configurations are (a) jet, (b) sheet, (d) film. The annular subconfiguration of sheets and films are shown in (c) and (e) respectively.

Figure 2: Generic diagrams illustrating the three regimes of jets in coflow—Rayleigh mode (a), Surface Breakup mode (b) and Prompt Atomization mode (c). The Surface Breakup mode diagram (b) represents a close-up view of the jet in that regime.

Figure 3: Generic diagrams illustrating the four atomization regimes for sheets—Sheet Pinching (a & b), Surface Breakup (c), Perforated (d) and Prompt Atomization (e). Sheet Pinching may occur in dilational (a) or sinusoidal (b) modes. The surface breakup figure (c) represents a close-up view of a portion of the sheet.

Figure 4: Impinging jets (a) and their subsequent behavior are similar to jets impacting splash plates (b). These two configurations also share several similarities with a jet impacting a wall (c), despite the lack of a sheet in the wall-impact configuration.

Figure 5: Effervescent atomizers operate with the nozzle flow in one of the following realms: bubbly (a), slug (b) or annular (c)

Figure 6: Generic diagrams illustrating the four atomization regimes for films—Ribbon Forming (a), Surface Breakup (b), Perforated (c) and Prompt Atomization (d). The Surface Breakup illustration (b) represents a close-up view of the film in that regime.

Figure 7: Large scale coherent gas-phase structures can, in some cases, affect the surface of a film. This illustration shows one way in which these structures can create disturbances. The spiral represents a clockwise-swirling vortex in the gas phase.

Figure 8: Ribbons may change shape due to aerodynamic effects as well as liquid-gas and liquid-solid surface tension. Here, the elongation of a ribbon due to aerodynamic enhancement is illustrated. The left figure shows a streamline in the gas and its curvature due to the ribbon.

Figure 9: Two types of breaking waves, spilling (a) and plunging (b), are shown just prior to breaking.

Figure 10: The profile of the film prior to and just after the rupture of the “bag” during bag breakup.

Figure 11: Ligament breakdown mechanisms including Rayleigh mechanism breakdown (b), base cutoff (c) and shattering (d) are shown along with the ligament prior to breakdown (a). Stripping examples are shown in Fig. 14.

Figure 12: Examples of stripping due to drag (a) and lift (b), i.e. variations in air pressure due to flow over the curved wave, are shown.

Figure 13: The result of a bubble rupturing is shown here in a cut-away view. The central created jet may or may not evolve to produce a droplet. The fine film droplets are not shown.

Figure 14: The three modes of droplet splashing are illustrated as well as the initial state prior to droplet impact (a). The modes are partial absorption (b), corona splash (b) and prompt splash (c).

Figure 15: Examples of the separation of film at a corner are given. The formation of a ligament is shown in part (a) and the formation of a sheet is shown in part (b).

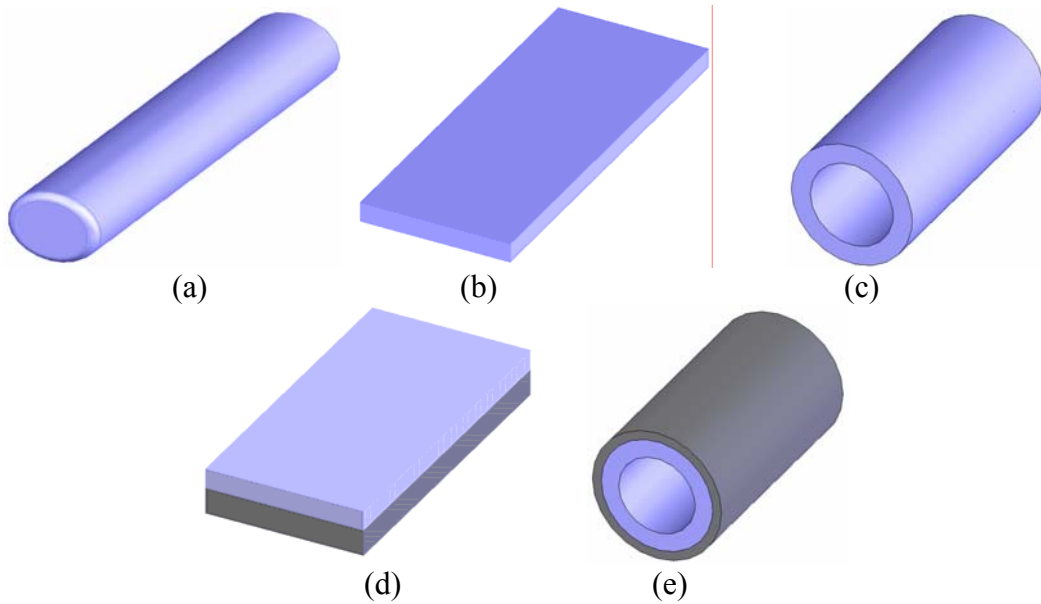


Figure 1

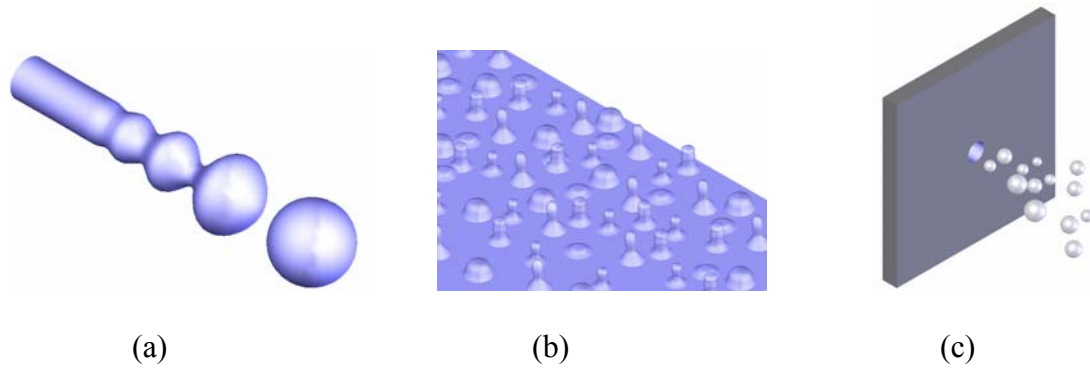


Figure 2

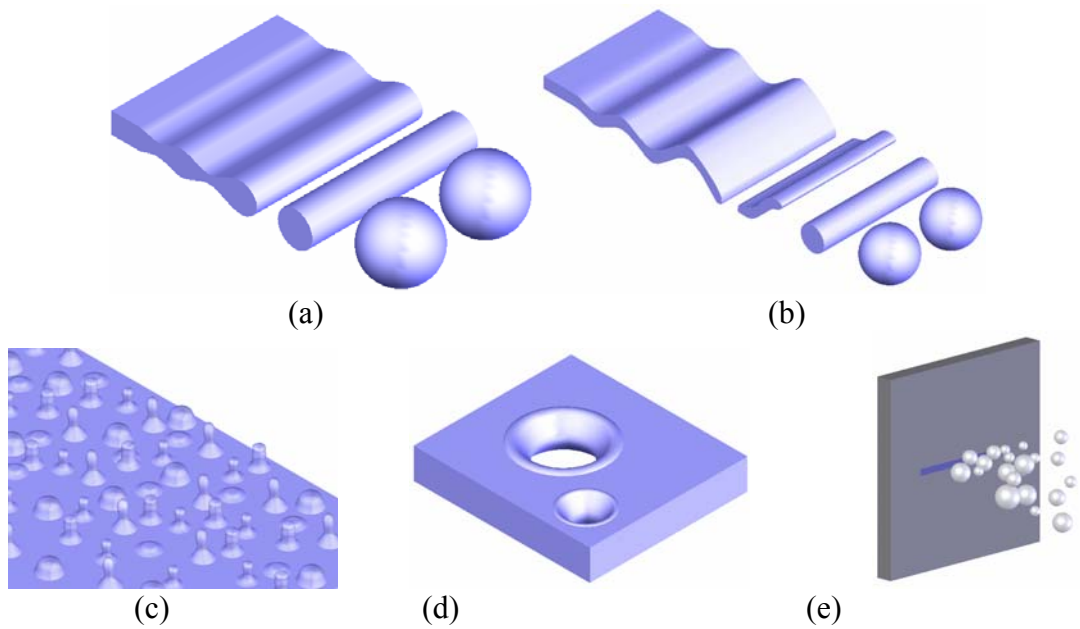


Figure 3

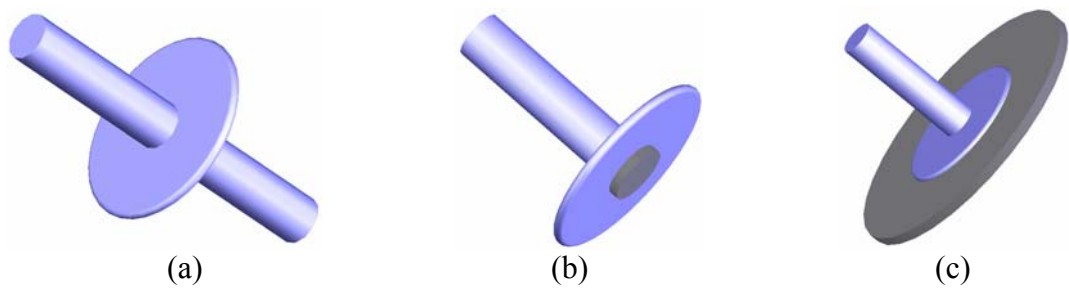


Figure 4

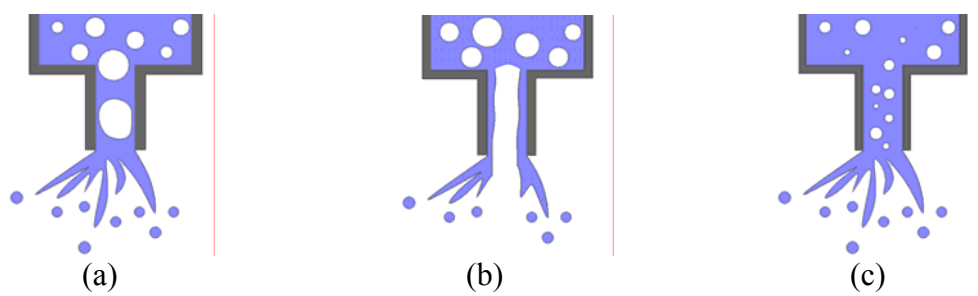


Figure 5

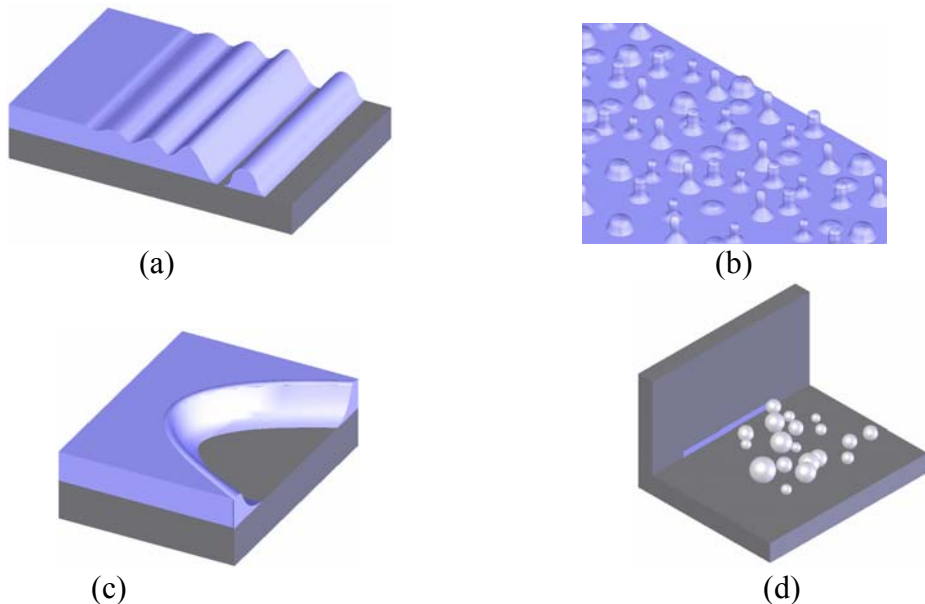


Figure 6

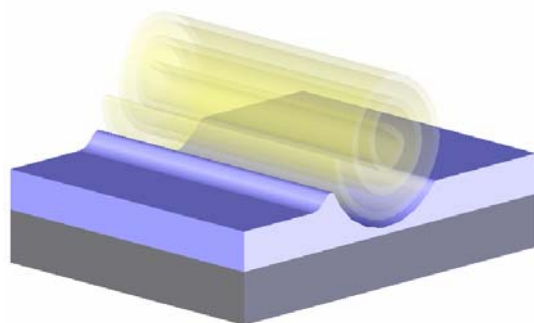


Figure 7

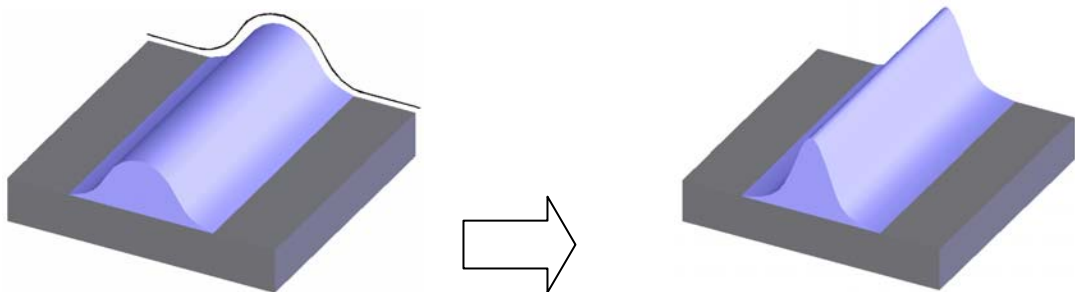


Figure 8

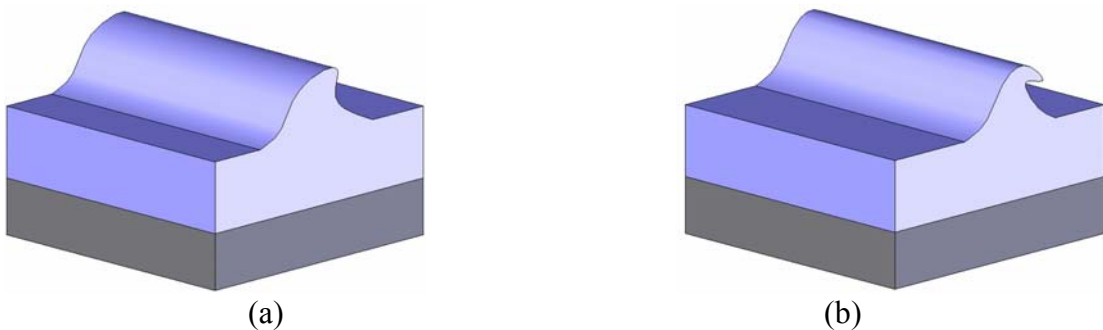


Figure 9

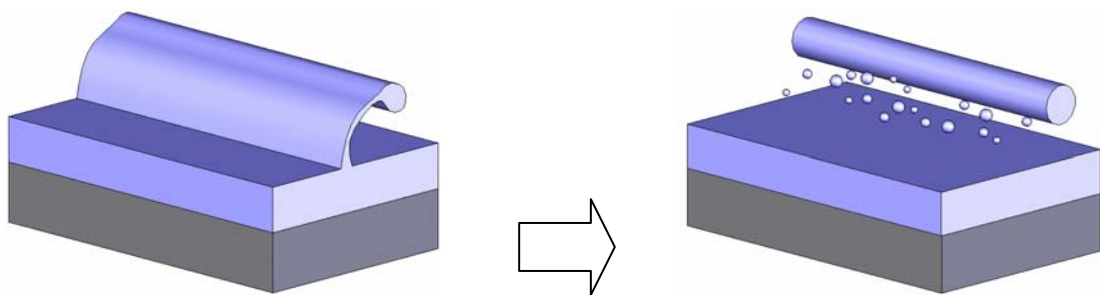


Figure 10

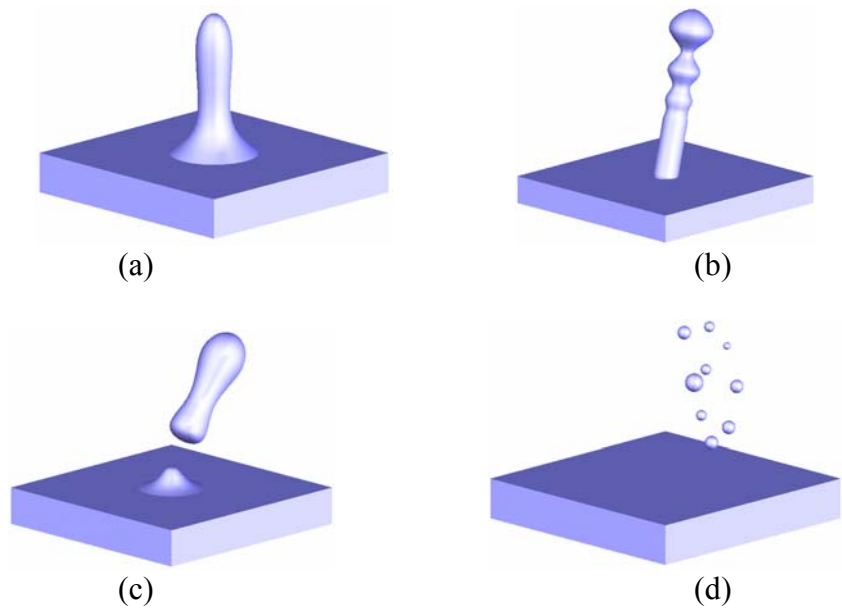


Figure 11

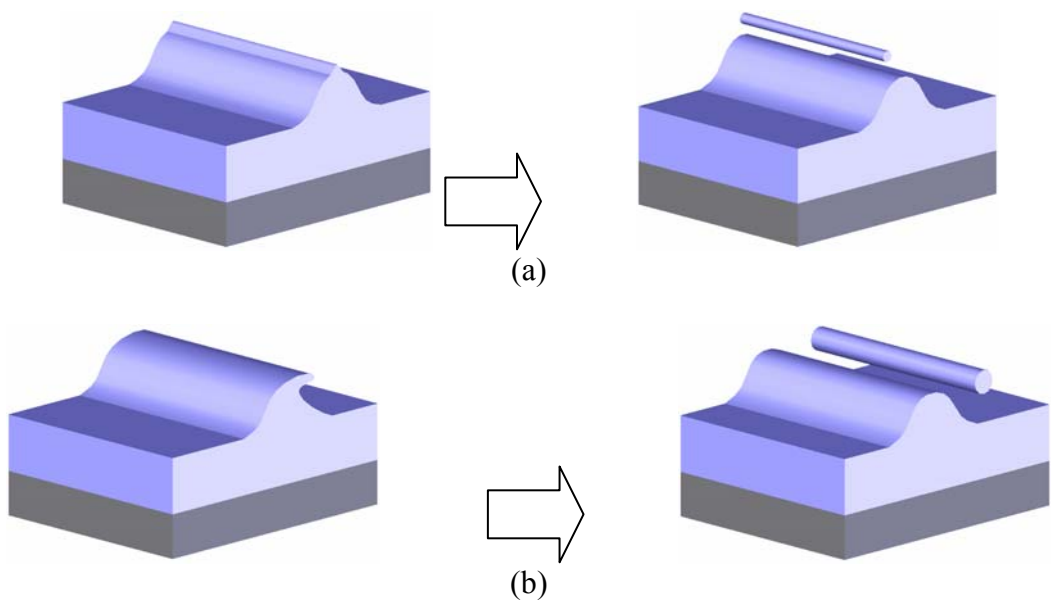


Figure 12

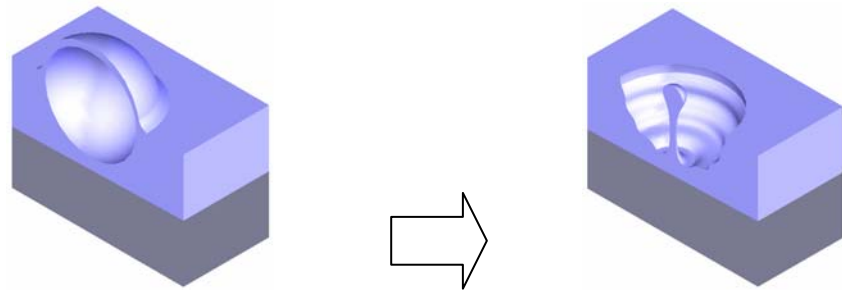


Figure 13

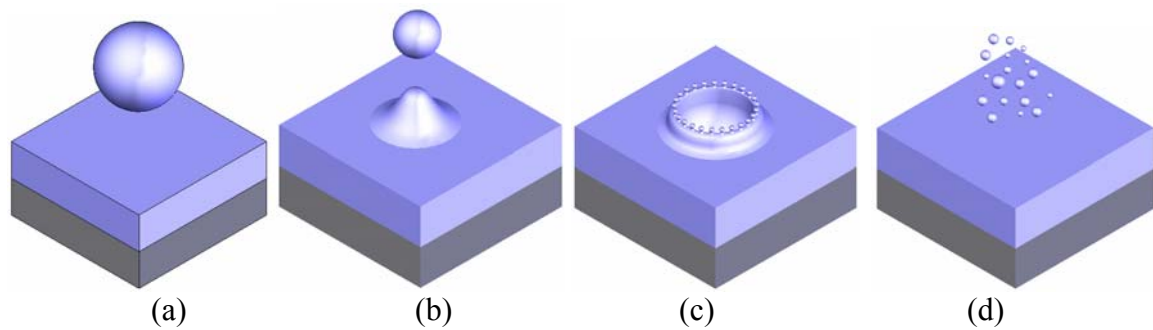


Figure 14

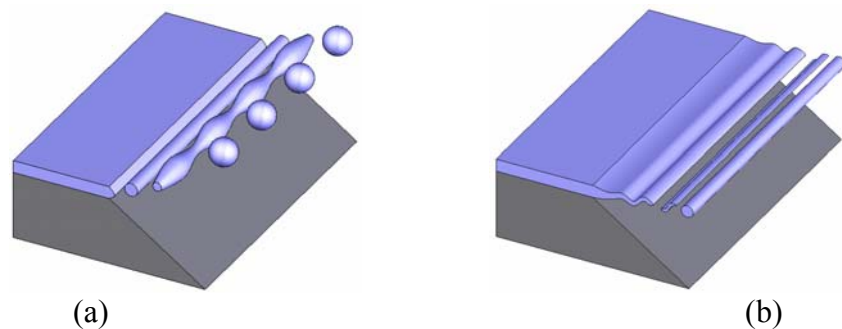


Figure 15